Dustiness Testing and Particle Characterization of CNT-enhanced Concretes

Sara Marsh

DIVISION OF ERGONOMICS AND AEROSOL TECHNOLOGY | DEPARTMENT OF DESIGN SCIENCES
FACULTY OF ENGINEERING LTH | LUND UNIVERSITY
2021

MASTER THESIS

Dustiness Testing and Particle Characterization of CNT-enhanced Concretes

Sara Marsh

Dustiness Testing and Particle Characterization of CNT-enhanced Concretes

Published by

Department of Design Sciences
Faculty of Engineering LTH, Lund University
P.O. Box 118, SE-221 00 Lund, Sweden

Subject: Aerosol Technology (MAMM05)
Division: Ergonomics and Aerosol Technology
Supervisor: Christina Isaxon
Examiner: Jenny Rissler

Abstract

The introduction of fibers into concrete is a common way of reinforcing the mechanical properties and preventing cracking. The fibers act as bridges between the composite components and help reduce the porosity. Today, micrometer-sized fibers are widely used, but there is an increased interest in using smaller fibers e.g. carbon nanotubes (CNTs), as they are able to stop smaller cracks and the initiation of cracks. These CNTs share structural similarities to asbestos fibers and they have been shown to cause increased risks of pulmonary diseases when inhaled. Therefore, the introduction of CNTs into any material requires life-cycle risk assessments. In this project, focus has been on characterizing the number and mass concentrations and size distributions of airborne emissions of crushed concrete in order to assess the dustiness. A continuous drop-method (according to EN 15051-3 standard) was setup in a controlled laboratory setting where three different crushed concrete-types were tested and the number and mass concentrations and size distributions were measured with both online instruments and filter sampling. Each concrete type was tested both without CNTs and with two different weight concentrations of CNTs in three replicates. The results show that the method is reproducible and that the CNTs could affect different concrete types differently, depending on both the concrete type and the CNT concentration. The concrete type with the lowest density and highest porosity (cellular lightweight concrete) resulted in the highest dustiness levels.

Keywords: concrete, dustiness, airborne particles, carbon nanotubes

Sammanfattning

Att tillsätta fibrer i betong är en vanlig metod för att förstärka de mekaniska egenskaperna och motverka sprickor i betongen. Fibrerna fungerar som broar mellan komponenterna i betongen och bidrar till att minska porositeten. Idag används vanligen mikrometerstora fibrer, men det finns ett ökat intresse för att använda mindre fibrer, exempelvis kolnanorör, eftersom de stoppa sprickorna i ett tidigare skede och motverka initieringen av sprickor. Kolnanorör delar strukturella likheter med asbestfiber och har kopplats till ökade risker för lungsjukdomar vid inandning. Därför krävs riskanalyser för hela livscykeln för material med tillsatta kolnanorör. I detta projekt har fokus varit på att karakterisera nummer- och masskoncentrationer och storleksfördelningar för luftburna partikelemissioner av krossad betong för att undersöka dammigheten. En kontinuerlig fallmetod (enligt EN 15051–3 standard) sattes upp i en kontrollerad laboratoriemiljö, där tre olika typer av krossad betong testades och nummer- och masskoncentrationerna samt storleksfördelningarna mättes med både direktvisande instrument och filtermätningar. Varje betongtyp testades både utan kolnanorör och med två olika viktkoncentrationer kolnanorör i tre replikat. Resultaten visade att metoden är reproducerbar och att kolnanoröreen kan påverka olika typer av betong på olika sätt, både beroende på betongsort och koncentrationen kolnanorör. Den betongtypen med lägst densitet och högst porositet (skumbetong) resulterade i högst dammighet.

Nyckelord: betong, dammighet, luftburna partiklar, kolnanorör

Acknowledgments

I would like to thank a number of people who have been a great help in this project.

Firstly, I would like to thank my supervisor Christina Isaxon for all the support and help with the project and Camilla Abrahamsson for all the hours spent in the lab.

I would also like to thank Jenny Rissler and Anders Gudmundsson for all the help with the experimental setup.

Thanks to Josef Forslund and the rest of the workshop at IKDC for producing the whole experimental setup and for being quick to help with all the changes.

Thanks to Monica Kåredal at AMM for all the help with the filter measurements and cyclones.

Thanks to Linnéa Jönsson for the SEM images.

Thanks to Ida Gabrielsson and Anna Bredberg at RISE in Borås for helping with the crushing of the concrete.

Last, but not least, I would like to thank my family and friends and especially Erik for all the support and love during the project.

Lund, September 30th

Sara Marsh

Table of contents

List of acronyms and abbreviations

APS	Aerodynamic Particle Sizer
CD	continuous drop
CLC	cellular lightweight concrete
CNT	carbon nanotube
CPC	Condensation Particle Counter
DMA	Differential Mobility Analyzer
IKDC	Ingvar Kamprad Design Centre
MCPC	Mixing-type Condensation Particle Counter
NSC	normal strength concrete
OC/EC	organic carbon/elemental carbon
OSHA	Occupational Safety and Health Administration
PM4	particulate matter with an aerodynamic diameter < 4 µm
RH	relative humidity
RISE	Research Institute of Sweden
SMPS	Scanning Mobility Particle Sizer
UHPC	ultra-high performance concrete

Sample types used in the project:

NSC 0	normal strength concrete without carbon nanotubes
NSC 0.05	normal strength concrete with 0.05 wt% carbon nanotubes
NSC 0.1	normal strength concrete with 0.1 wt% carbon nanotubes
CLC 0	cellular lightweight concrete without carbon nanotubes
CLC 0.1	cellular lightweight concrete with 0.1 wt% carbon nanotubes
CLC 0.3	cellular lightweight concrete with 0.3 wt% carbon nanotubes
UHPC 0	ultra-high performance concrete without carbon nanotubes
UHPC 0.3	ultra-high performance concrete with 0.3 wt% carbon nanotubes
UHPC 0.5	ultra-high performance concrete with 0.5 wt% carbon nanotubes

1 Introduction

1.1 Research question

Concrete is one of the most common construction materials in the world. It has a high compressive strength, but low flexural and tensile strength. Since concrete structures are often exposed to detrimental processes such as heating, freezing, corrosive chemicals, wearing or uneven loading, the demand for increasingly stronger and more durable construction materials is high (Baloch, 2018). One common way to reinforce the concrete and control cracking is to introduce fibers into the concrete. Fibers widely used are organic (e.g. polymers like polypropylene), inorganic (e.g. glass and carbon) and cellulose (Hu, 2013) and they typically range from micrometers to centimeters in length. The fibers can act as bridges between the different composite components in the concrete and help reduce the porosity, while improving the mechanical properties (Hu, 2013; Lu, 2016; Xu, 2015). They are not as effective at improving the tensile strength as reinforcing steel bars, but since they are more finely dispersed they are better at preventing crack propagation (Chan, 2010). Cracks can be destructive for concrete structures, not only due to a reduction in strength, but also through letting in corrosive elements (such as water, oxygen, carbon dioxide and sulfate ions) that reach the reinforcing steel bars embedded in concrete (Lim, 2017). Micrometer-sized fibers are able to inhibit the propagation of macro-sized cracks, but not able to inhibit smaller cracks or stop the initiation of cracks (Hu, 2013; Baloch, 2018). Therefore, there is an increased interest in using smaller, i.e. nano-sized, fibers such as carbon nanotubes (CNTs).

CNTs are interesting due to their exceptional mechanical, electrical and thermal properties and have already been used for reinforcing polymer composites (Gupta, 2018). The addition of CNTs could prevent the initiation of cracking and studies have shown that they can improve the mechanical strength and durability of cement composites. Yakovlev et al. showed that an addition of 0.05 wt% of CNTs into a foam concrete improved the compressive strength by up to 70 % (Yakovlev, 2006). Yang et al. showed that an addition of 0.1 wt% CNTs into a cement-based material increased the impermeability resistance and abrasion resistance (Yang, 2014). Konsta-Gdoutous et al. showed that adding 0.08 wt% of CNTs into cement paste increased the flexural strength by 35 % (Konsta-Gdoutous 2010). There are also reports of CNTs improving the electrical properties of concrete which could enable a concrete composite to also function as a crack sensor. Lim et al. reported that cracks in the concrete could be sensed by measuring a decrease in the concrete/CNT conductivity (Lim, 2017). It is not fully known how common the use of CNT-enhanced concrete is today, but it is likely to increase since a lot of research and development is going on.

Due to the high aspect ratio of the CNTs (much like asbestos fibers), there could be risks associated with the exposure of the material, mainly through inhalation. The small diameter of the fibers enable them to reach deep into the lung, where the body's clearance systems might not be able to clear them. Therefore, the introduction of CNTs into any material also requires a risk assessment of the whole life-cycle impact, from production, application and workplace exposures to waste management. There are studies of the exposures from the production step of CNTs, but more research is needed on the exposures from handling CNTs at workplaces (Kujipers, 2015).

In this project, the main focus has been on characterizing the airborne emissions, in regards to number and mass concentration and size distribution, of crushed concrete during handling in a laboratory setting. A method was set up for simulating the dustiness at workplace scenarios, where there is a risk for dust being aerosolized by air currents.

1.2 Challenges

Since the propensity of the crushed concrete to become aerosolized depends on a number of factors such as humidity and agitation mechanism, this needs to be considered when choosing the method for dustiness testing. It is also difficult to measure and quantify the carbon nanotubes in the aerosol as they might be free or agglomerated particles or encapsulated in the concrete matrix. In general, it is difficult to measure engineered nanoparticles in occupational settings as the background often contains naturally occurring nanoparticles.

1.3 Aims

The aims of this project were to:

- Choose a method and design and fabricate an experimental setup to in a safe way measure and characterize concrete dust with regards to number and mass concentrations and size distribution, in a reproducible way in a laboratory setting.
- Characterize the emitted airborne particles for three different types of concrete without carbon nanotubes and with different concentrations of carbon nanotubes, to see how the particle emissions, size distributions and dustiness levels differ between concrete types and carbon nanotube concentrations.
- Investigate how the carbon nanotubes appear in the aerosol particles: as free particles, agglomerates or embedded in the concrete and quantify the amounts of carbon nanotubes in the aerosol compared to the bulk material.

2 Theory

An aerosol is defined as a suspension of liquid or solid particles in a gas, the most common being air. The aerosol particles are called particulate matter (PM) and different size fractions can be of interest in different applications.

The sizes of aerosol particles range from a few nanometers to around 100 µm in diameter. There is no real lower size limit as a particle is defined as a small discrete object. The upper size limit can be determined by the settling velocity, which depends on the particle diameter and density. As airborne particles can vary greatly in shape, the diameter of a particle is usually described in equivalent diameters, which is the effective diameter of a particle depending on a specific measurable property. For instance, the aerodynamic diameter depends on the settling velocity while the mobility equivalent diameter depends on the particle's velocity when subjected to an external force, like an electric field. (Kulkarni, 2011)

Apart from size and shape there are other important factors that affect the aerosol behaviour. The particle concentrations and size distributions can be characterized based on different parameters, most commonly by number, mass, surface area or volume. Many small particles can contribute a lot to the number concentration while contributing little to mass concentrations.

2.1 Aerosol size fractions

When evaluating possible health risks of airborne particles it is important to assess to what degree and where different particles deposit in the respiratory tract system. The possible health effects could be linked to only a fraction of the aerosol, depending on the particle properties and the human respiratory system. For instance, coal mine dusts that reach the lung can cause pneumoconiosis and silicosis while a larger fraction of the dust can cause bronchitis and reduce pulmonary function (Brown, 2013). Therefore it is not always the best representation to sample the total aerosol concentration. Instead, it is common to use size-selective sampling that only samples the particle sizes relevant for a specific deposition site in the respiratory tract system (Brown, 2013).

The human respiratory system can be divided into three main regions: the head, the tracheobronchial region and the alveolar region. These same regions can be used when defining the different aerosol fractions, see Figure 2.1. Although particle deposition and clearance varies between different individuals, it is still meaningful to define a standard convention to better understand health risks associated with inhaled particles. The European Committee for Standardization (CEN) has defined main aerosol mass fractions for this purpose: (CEN, 1993).

- Inhalable fraction: <100 µm
  The particles that are inhaled through the nose and mouth.
- Thoracic fraction: <10 µm
  The particles that reach beyond the larynx, into the ciliated airways
- Respirable fraction: <4 µm
  The particles reaching the unciliated airways.

The size limits are defined using the aerodynamic diameter and are based on the particles with a 50 % penetration efficiency relative to the total aerosol (Brown, 2013).

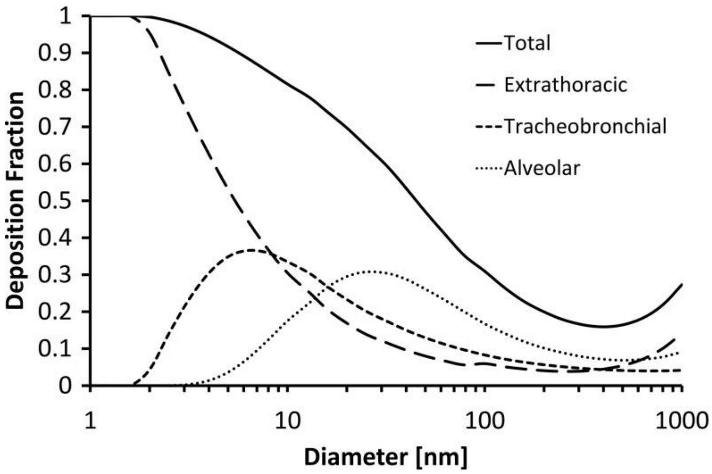

Figure 2.1 Lung deposition curves for different aerosol fractions. Source: (Löndahl, 2014).

2.2 Carbon nanotubes

Carbon nanotubes (CNT) are tubular high aspect ratio structures of rolled up graphite sheets, a planar honeycomb elemental carbon structure. They can be either single-walled (SWCNT) or multi-walled (MWCNT). Single-walled are typically 1-2 nm in diameter and multi-walled are typically 10-20 nm in diameter. The lengths can vary greatly, usually from hundreds of microns up to centimeters (Popov, 2004; Dai, 2002).

CNTs have exceptional mechanical, thermal and electronical properties and are one of the most resilient materials (Dai, 2002). They have been shown to have a very high Young's modulus, which is a measure of the stiffness of a material, in the order of 1 TPa, while other carbon fibers typically have 680 GPa. They also have a very high tensile strength, up to 100 times the strength of steel, with a much lower density (Dai, 2002). This means they can endure high strains before mechanical breaking. They have also been proven to have a very high thermal conductivity and are thermally stable up to 2800 ℃ in vacuum (Thostenson, 2001). Their electrical properties depend on the structure and they can be both metallic or semiconducting (Dai, 2002).

2.2.1 **Toxicity**

There are a number of reasons for studying the toxicity of carbon nanotubes. Nanoparticles in general tend to possess different properties than larger particles of the same material, for example due to the high surface-to-volume ratio which can enhance the reactivity. For instance, materials that are nontoxic or catalytically inactive in bulk can become toxic or catalytic when produced at the nanoscale (Modena 2019; Viitanen, 2017). There is also the morphological resemblance of CNTs to asbestos fibers, which have been shown to induce adverse health effects in human lungs and mesothelium. (Donaldson, 2010). A third interesting property of CNTs is that they are possibly biopersistent, due to their graphitic nature. (Donaldson, 2006)

There are four important characteristics when assessing fiber toxicity: (Sanchez, 2009)

- Size and shape – the deposition mechanism and efficiency depends on the particle length, width, shape and density. A particle with an aerodynamic diameter > 5 µm tends to deposit due to impaction, when there is a sudden directional change in the airflow, usually in the upper respiratory tract. Particles with an aerodynamic diameter < 5 µm tend to deposit due to diffusion, deeper in the respiratory system.
- Biopersistence – if the particles are not effectively cleared by the body’s clearance mechanisms they are deemed to be biopersistent and the amounts will accumulate over time.
- Surface properties and reactivity – CNTs are hydrophobic and difficult to disperse in aqueous environments. They are often surface treated to change the functionality, which can make them more reactive to cell receptors and affect biological responses. They can also adsorb macromolecules or other smaller molecules and thereby impact biological systems. They often contain residual redox-reactive transition metals that are used as catalysts for CNT production and that have been linked to human cancer.
- Agglomeration – CNTs tend to agglomerate and the toxicological consequence is not precisely known.

Animal inhalation studies have linked MWCNT exposures to diseases including pulmonary fibrosis, lung cancer and mesothelioma, risks also associated with asbestos exposure (Ellenbecker, 2018).

2.3 Workplace emissions and exposures

Today there is little data available on the health effects from exposure of engineered nanoparticles among workers. The data available are mainly focused on small-scale exposure from research and development and not larger scale exposures from the manufacturing processes. Therefore, more research is needed to study the effects of normal use and more occupationally relevant exposure levels.

In order to assess the risks of a material, it is necessary to study both the exposure and the toxicity. The first stage to determine the exposure is to characterize the emitted aerosol particles from the material in regards to particle size distribution and number and mass concentration. However, the emitted aerosol is not necessarily the same as the aerosol that is later inhaled, since the particles will travel through the air and interact with other particles. This can change the particle size distribution and number concentrations (Seipenbusch, 2008)

There is also the challenge of measuring and characterizing specific engineered nanoparticles with a polydisperse background containing ambient nanoparticles. This is one reason for carrying out emission studies in a controlled laboratory setting.

2.4 Dustiness measurements

The dustiness of a material can be defined as the "propensity of a powder to generate airborne dust during its handling" (Liden, 2006) and this is an important component when determining the health and safety risks involved with powder materials. However, the dustiness is not an intrinsic property of the dust. It also depends on factors such as air humidity, turbulence, adhesion forces and the agitation method (Liden, 2006; Klippel, 2015). This means that the dustiness will depend on the measurement method, which complicates standardization and comparisons of powder materials. It is therefore important to choose a method that simulates the relevant conditions that are meant to be assessed. Three aspects are especially important to keep in mind when determining the most appropriate test method:

1. To sample the biologically relevant aerosol fractions: inhalable, thoracic and respirable fractions.
2. To use an applied mechanical force that resembles the material handling at the workplace.
3. To relate the measured dustiness results to the generation strength of the dust source at the workplace.

This has resulted in a number of test methods that can be used to simulate different situations, by using different agitation methods for instance. (Liden, 2006)

2.4.1 The continuous drop method

There are two methods for measuring dustiness that are explained by a European standard, EN 15051. The methods use different agitation techniques and therefore cover different workplace scenarios.

One of those methods is the continuous drop method and it is based on the dropping of a powder material in a cylinder with a backflow of air that aerosolizes particles. The powder is continuously fed with a metering device in order to maintain an even, steady flow. The powder drops down by gravity in an inert cylinder with the dimensions of 1100 mm in length and 150 mm in diameter. The backflow will bring along aerosol particles that are sampled at different aerosol fractions, inhalable and respirable. There is a collector tank at the bottom of the main cylinder that collects the material that is not aerosolized and this is used for gravimetric analysis, where the sampled aerosol fractions are compared with the not-aerosolized material. The sample outlets can be connected to different filters and online measurement devices in order to determine number concentrations and size distributions or any other aerosol property of interest.

The continuous drop method can be used to simulate workplace scenarios where there is falling or winnowing of dust or when dust particles are being aerosolized by air currents.

2.4.2 Measurement and analysis techniques

Different aerosol measurement techniques are often applied when characterizing aerosols due to the different detection size ranges of the instruments. Different instruments also detect different particle properties. There are two main approaches: filter sampling for later analysis or online reading instruments. Both online and offline sampling was done in this project and the online instruments used are listed and explained below.

2.4.2.1 Aerodynamic particle sizer (APS)

An APS measures the particle velocity relative to the air velocity in order to determine the size of the particle. The aerosol is passed through a nozzle that accelerates the flow. The time of flight of the aerosol particle is measured with the light scattering between two pulses of light. A large particle will have a lower velocity relative to the air velocity as it lags behind due to inertia. This data is used by the instrument to derive the particle number concentration by size. (Kulkarni, 2011)

2.4.2.2 Scanning Mobility Particle Sizer (SMPS)

An SMPS consists of two parts: one differential mobility analyzer (DMA) and one condensation particle counter (CPC). The DMA separates aerosol particles by the mobility equivalent diameter and produces a monodisperse aerosol. It is often a cylinder with a laminar sheath flow of clean air surrounded by a thin layer of polydisperse aerosol. (Hinds, 1999) The particles are charged and a central rod with an applied voltage will make the particles travel from the outer layer towards the center. Only the particles with the right electrical mobility will exit through the outlets. Particles with a higher mobility travel to the center too early and are deposited onto the center rod while particles with a lower mobility do not travel far enough and exit with the sheath flow or are deposited. (Kulkarni, 2011)

The CPC measures nanoparticles that are normally too small to be detected optically. The CPC uses supersaturation of a vapor (usually water or an alcohol) to make the nanoparticles grow into a micrometer size range where they are able to be detected optically. This technique preserves the number concentration of the aerosol. One type of CPC is the mixing-type CPC (MCPC). It combines two different aerosol streams of different temperatures, usually one with saturated vapor and one with the sample aerosol. This technique has a faster response and a very small diffusion loss of particles due to the short aerosol delivery distance. (Kulkarni, 2011)

An SMPS combines a DMA and CPC in order to determine the number particle concentration and particle size distribution. The voltage in the DMA is scanned in order to sort particles of different sizes. The CPC receives the monodisperse aerosol from the DMA and determines the particle number concentration at that size. (Kulkarni, 2011)

2.4.2.3 DustTrak (DT)

The DustTrak is a portable device that measures mass concentrations using laser photometers in different fractions: PM10, PM4, PM2.5, PM1 and the total fraction.

2.4.2.4 NanoTracer (NT)

The NanoTracer is also portable and measures number concentrations by charging particles and measuring the electrical current produced (Marra, 2010), with a detection range of 10-200 nm in particle diameter.

2.4.2.5 OC/EC analysis

OC/EC analysis is a method used for analyzing elemental carbon and organic carbon contents by heating a filter sample in an inert atmosphere.

2.4.2.6 Scanning electron microscopy (SEM)

The SEM uses an electron beam to scan the surface of a sample and forms images from the scattered electrons at very high resolutions, at the nanoscale (Zhou, 2006).

3 Method

3.1 Preparation of concrete

3.1.1 The concrete samples

The experiments included three types of concrete, with and without added CNTs. The three types were normal strength concrete (NSC), cellular lightweight concrete (CLC) and ultra-high performance concrete (UHPC). Each type was tested without CNTs and with two different concentrations of CNTs.

UHPC has a high density which leads to a very high strength, up to six times the strength of normal concrete, and high durability due to the low permeability. It is used for a variety of applications such as lightweight roofs, bridges and repair of damaged concrete. The possibility to produce lightweight structures with the highly dense concrete stems from the need for less material due to the high mechanical performance. (RISE, Ultra-high Performance Concrete, n.d.)

CLC is a low density concrete achieved by an introduction of foam to the cement paste. The density usually ranges from 120-2 000 kg/m^3 and the mechanical strength decreases with the decrease in density, due to the higher porosity. CLC has very good insulating properties and is often mixed with fibers or other concrete types to counter the low mechanical strength. (RISE, Cellular lightweight concrete, n.d.)

The NSC is of intermediate strength and density and contains cement, water and ballast (often sand or stone).

The concrete used was provided by the Research Institute of Sweden (RISE) in Borås. The density and CNT concentrations of each concrete type is shown in Table 3.1.

The carbon nanotubes are multiwalled of the type NC7000™ with an average diameter of 9.5 nm and an average length of 1.5 µm. Their carbon structure purity is 90 % and they contain < 1 % transition metal oxides. They are produced by Nanocyl in Belgium, by catalytic chemical vapor deposition (Nanocyl, (n.d.).

Table 3.1 Concrete types with their respective CNT weight concentrations and densities.

Concrete type	Fraction of CNTs (wt%)	Density (kg/m^3)
NSC	0	2187
	0.05	
	0.1	
CLC	0	300
	0.1	
	0.3	
UHPC	0	2350
	0.3	
	0.5	

3.1.2 Crushing concrete

The concrete containing CNTs was crushed with a Jaw Crusher BB 250 XL, before the start of this project, at the RISE facility in Borås in February 2020. The concrete without CNTs was crushed in March 2021, at the same facility using the same equipment to ensure as similar crushing process as possible, see Figure 3.1. The CLC and UHPC without CNTs were from the same batches as the concrete containing CNTs, but the NSC was of a different batch but with similar composition.

Figure 3.1 Crushing of concrete.

3.1.3 **Sifting concrete**

All of the concrete was sifted in the aerosol lab at IKDC with a 0.850 mm sieve (see Figure 3.2). This size was selected in order to remove the largest concrete pieces that could clog the aerosolization mechanism in the continuous drop-setup, while still keeping enough material to be able to conduct the experiments.

Figure 3.2 Sifting concrete, 0.850 mm.

3.1.4 **Conditioning of concrete**

In order to condition the concrete samples they were kept in open ziplock bags in the aerosol exposure chamber for a minimum of 24 hours before testing. This was to ensure similar humidity in the different samples.

3.2 The setup

3.2.1 **Chamber parameters**

The aerosol exposure chamber is a chamber with a volume of 21.6 m^3 and the ability to control air temperature, relative humidity (RH) and air exchange rate. It has floors and walls of stainless steel with openings for instrument sampling and an air lock for safe entering and exiting.

An underpressure of 5-10 Pa was kept in the chamber in order to avoid aerosol particles leaking out of the chamber into the rest of the lab. The air exchange rate in the chamber was set to 11.0 h^{-1} to establish efficient clearance of any particle leakage inside the chamber and to minimize the exposure for the operator.

3.2.2 The continuous drop method

The setup for the CD-method is shown in Figure 3.3. It is made up of a main cylinder of stainless steel with 150 mm in diameter and a length of 1 100 mm. Inside the main cylinder is the inner tube with a diameter of 25 mm that extends 400 mm down into the main cylinder. The crushed concrete is placed in the top container and is rotated by a rotating arm that pushes the crushed concrete towards an opening with 2 mm in diameter. The opening connects to the inner tube where the crushed concrete falls down through the main cylinder to a container at the bottom.

Through the main cylinder is an upwards directed air flow that is set to 53 l/min in total, according to the EN 15051-3 standard. This backflow comprises the main flow that is controlled by an external pump and the flows from the sampling instruments. There are six sampling outlets that are placed 800 mm from the bottom and thereby 100 mm above the lower opening of the inner tube. The sampling tubes are mainly stainless steel and short tygon tubes in order to minimize deposition of particles.

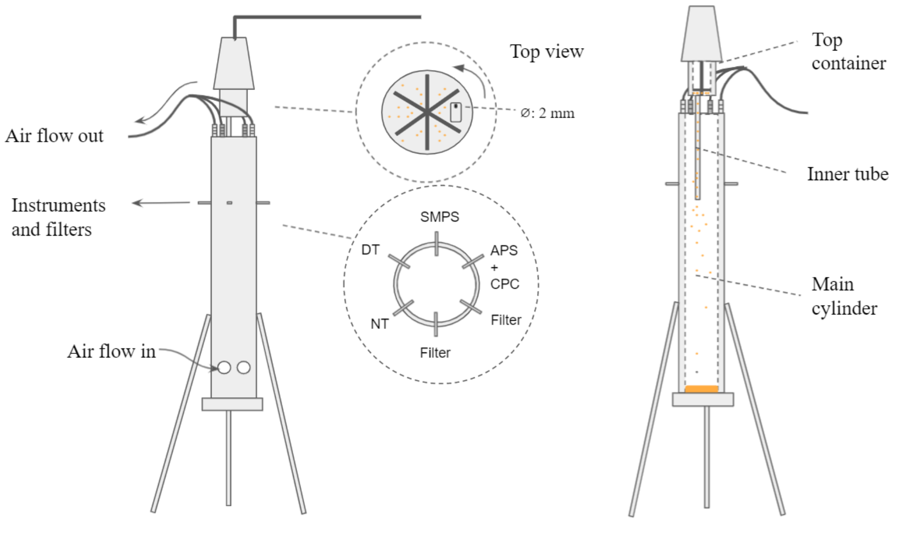

Figure 3.3 Schematic of the continuous drop setup. Figure provided by Camilla Abrahamsson.

The testing is started when the backflow pump and rotating arms are started, simultaneously. The filter sampling started after two minutes, to avoid transient processes at the start. The total testing time was 10 minutes in the EN 15051-3 standard, but here set to 15 minutes for the online instruments and 13 minutes for the filters. This was to ensure that enough particles were sampled on the filters after the delayed start.

3.2.3 Instruments and sampling parameters

The online instruments that sampled the aerosol and their sampling parameters are listed in Table 3.2. The sampling flows for each instrument were measured before the testing of each concrete type. The background concentration in the chamber was also measured using a CPC, here called background CPC.

Table 3.2 Instruments and sampling parameters.

Instrument	Sampling flow (l/min)	Sample time resolution (s)	Detection range (nm)
APS	1.2	5	500 – 20 000
SMPS	0.3	90 + 20*	15 – 650
MCPC	0.8	3	7 – 2 000
DT	3.0**	1	PM4
NT	0.4	10	10 – 300
Background CPC	1.0	1	5 – 2 500

*90 s scan time + 20 s purge time
**2 l/min measured aerosol flow + 1 l/min sheath flow

There were four filter types sampled: teflon filters for both total and respirable fraction for gravimetric analysis, polycarbonate filters for SEM analysis and quartz filters for OC/EC analysis. Blank filters were also used for reference.

The gravimetric filters were sampled for each test and the SEM and OC/EC filters were only sampled once for each concrete type and CNT concentration. The sampling flow was 2.2 l/min for each filter. The PM4 and OC/EC filter samples were mounted on PM4 cyclones, that required a 2.2 l/min inlet flow for the correct cutoff diameter. The Total and SEM filters were not mounted onto cyclones and therefore sampled the whole aerosol. The filter samples flows were measured before and after each test.

The flow to the backflow pump was set to 38 l/min and was measured before testing each concrete type.

3.2.4 **Evaluation of dustiness**

The respirable dustiness mass fractions (w_R) are calculated with Equation 1 from the EN 15051-3 standard.

$$w_R = \frac{\Delta m_R}{m_C} \frac{Q_{tot}}{Q_R} \tag{1}$$

Δm_R is the sampled respirable filter mass in milligrams, m_C is the collected mass in the bottom container in kilograms, Q_{tot} is the total air flow rate up through the main cylinder, Q_R is the flow rate of the respirable filter sampling.

The dustiness mass fractions are classified in the EN 15051-3 standard in four categories: “very low”, “low”, “moderate” and “high”, see Table 3.3. The categories are based on the quartiles of the results of dustiness testing of more than 500 different materials.

Table 3.3 Dustiness classification categories from the EN 15051-3 standard.

Dustiness category	**Respirable dustiness mass fraction w_R, (mg/kg)**
Very low	< 20
Low	20 to 70
Moderate	> 70 to 300
High	> 300

3.2.5 **Risk management**

Due to the potential toxicity of CNTs a thorough risk management was conducted before the initiation of the experiments, see Appendix F. The background number concentrations were also measured in the exposure chamber for operator safety, the graphs are available in Appendix E.

The personal protective equipment used in the lab experiments were disposable shoe covers, protective clothing (reusable overalls), disposable nitrile gloves, respirator with P3 R particle filter and protective glasses.

4 Results

Nine experiments in three replicates each were conducted in order to compare the dustiness of different concrete types and different concentrations of CNTs and assess the reproducibility of the method. Different online instruments, that measure different particle properties and different particle size ranges, were used as well as offline filter sampling of the total and respirable fractions for gravimetric analysis and SEM analysis.

The number concentrations, mass concentrations (both from online instruments and gravimetric filter sampling), number average size distributions, dustiness and SEM images were assessed. Filter samples for OC/EC analysis were also collected, but not analyzed within this project. All the data from the online instruments are presented in Appendix A.

4.1 Continuous drop methodology

The average concentrations and standard deviations of the replicates were calculated in order to assess the reproducibility of the continuous drop setup. For one test, the normal strength concrete with 0.1 wt% CNTs, only two replicates were done due to a limited material supply. The average concentrations from the APS data had the lowest noise levels and the results are shown in this chapter. The average concentrations from the other instruments are listed in Appendix C and are in line with the APS measurements.

The chamber was continuously conditioned with virtually particle-free air and the background concentration in the chamber was monitored during and in between testing.

4.1.1 Test-to-test variations in mean number concentrations

Figure 4.1 shows the test-to-test variation of the mean number concentrations for the experiments with the NSC with two different concentrations of carbon nanotubes as well as the NSC without carbon nanotubes. The results show a small variation between tests and the error bars indicate one standard deviation.

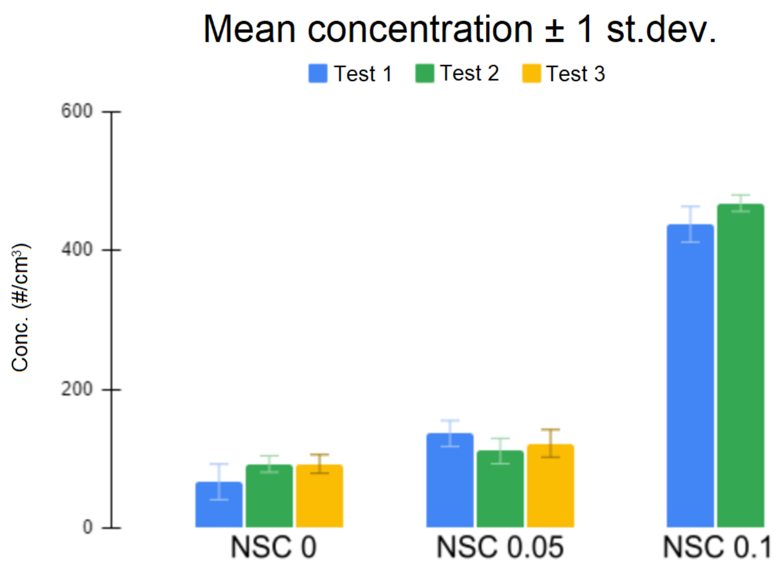

Figure 4.1 The mean concentrations from the APS data for the normal strength concrete. The error bars show one standard deviation.

The CLC also showed insignificant variations between replicates, see Figure 4.2.

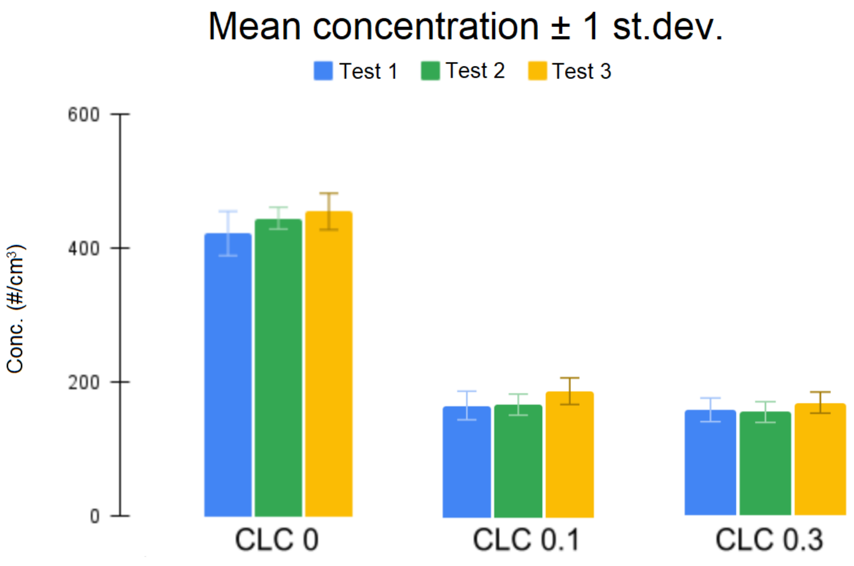

Figure 4.2 The mean concentrations and standard deviations from the APS data for the cellular lightweight concrete.

The UHPC mean number concentrations from the APS are shown in Figure 4.3. The test-to-test variation was higher for the concrete with CNTs.

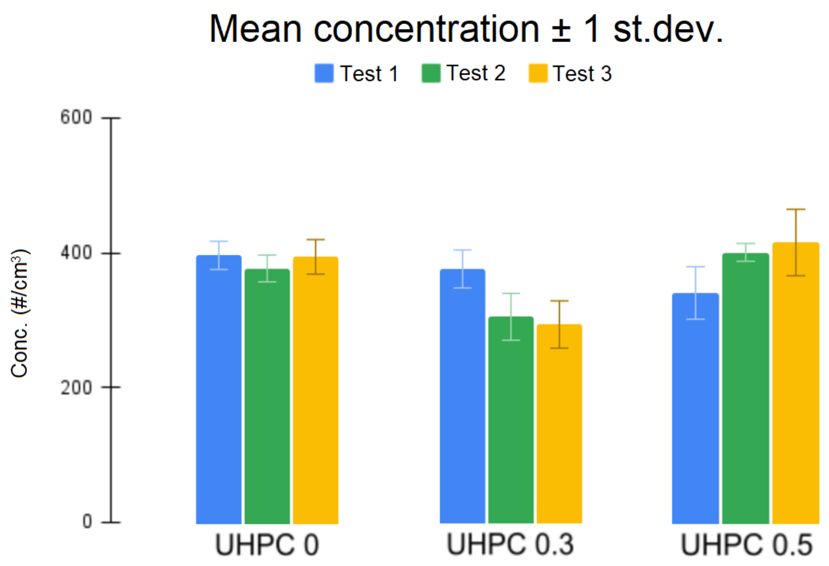

Figure 4.3 The mean concentrations and standard deviations from the APS data for the ultra-high performance concrete.

4.1.2 **Potential sources of error**

In the continuous drop experiment the crushed concrete mass that fell down from the top container also varied between tests. Both the fallen mass and the retained mass were weighed and the results are presented in Appendix B. During the collection and weighing of the fallen and retained crushed concrete, there was some spill due to the method of transferring the material, which affects the resulting mass balance.

The mass flow rate of the crushed concrete was ten times lower than in the EN 15051-3 standard, due to the mechanism of the rotating arms and the 2 mm opening in the top container. Attempts were made to achieve a higher mass flow rate by using a 3.5 and a 4 mm opening instead, but this resulted in unstable aerosol concentrations and a non-continuous drop pattern of the crushed concrete, as most of the material fell down during the first minutes.

The setup was placed inside the exposure chamber with temperatures ranging from 21.6 °C to 30.5 °C and a relative humidity ranging from 20.7 % to 40 %. The target values from the EN 15051-3 standard were 21 ± 3 °C and 50 ± 10 % RH. The deviations from the standard were caused by malfunctioning of the chamber climate control.

4.2 Concrete dustiness

The respirable dustiness mass fractions, w_R, were calculated according to Equation 1 for both the used sifted material and for the total amount of material. The results are presented in Table 4.1. The sifted material made up 29-36 % of the NSC total mass, 88-97 % of the CLC total mass and 32-42 % of the UHPC total mass. These fractions were used to calculate the w_R for the total material.

Table 4.1 Calculated respirable dustiness mass fractions, w_R, and dustiness classifications for the different concrete types, for both the sifted material and the total material.

Sample type	w_R sifted material (mg/kg)	Dustiness category	w_R total material (mg/kg)	Dustiness category
NSC 0	181	Moderate	65	Low
NSC 0.05	189	Moderate	55	Low
NSC 0.1	254	Moderate	84	Moderate
CLC 0	223	Moderate	197	Moderate
CLC 0.1	117	Moderate	111	Moderate
CLC 0.3	170	Moderate	165	Moderate
UHPC 0	254	Moderate	81	Moderate
UHPC 0.3	174	Moderate	70	Low
UHPC 0.5	238	Moderate	100	Moderate

All the concrete types fall under the “moderate” dustiness category when only the sifted material is assessed. When the total amount of material is taken into account, the CLC shows higher dustiness levels than the other concrete types with all three samples in the “moderate” category. The UHPC has the second highest dustiness with two samples in the “moderate” category and one in the “low” category. The NSC shows the lowest dustiness with one sample in the “moderate” category and two samples in the “low” category. The CLC has the highest dustiness for the concrete without CNTs, while the NSC and UHPC has the highest dustiness for the concrete with the highest concentration of CNTs. All three concrete types have the lowest dustiness for the sample with the lowest concentration of CNTs.

4.2.1 **Size distributions**

The number size distributions of the aerosol particles were measured with the SMPS and APS and showed three main patterns. They were either bimodal or trimodal within the measured size range (15 – 20 000 nm). The size distribution graphs presented in this chapter and in Appendix A show the average distribution over the total sampling time.

The first, most common pattern was a bimodal distribution with one peak at around 170 nm and another at around 2 µm. Figure 4.4 shows the bimodal size distribution for the CLC with 0.3 wt% CNTs.

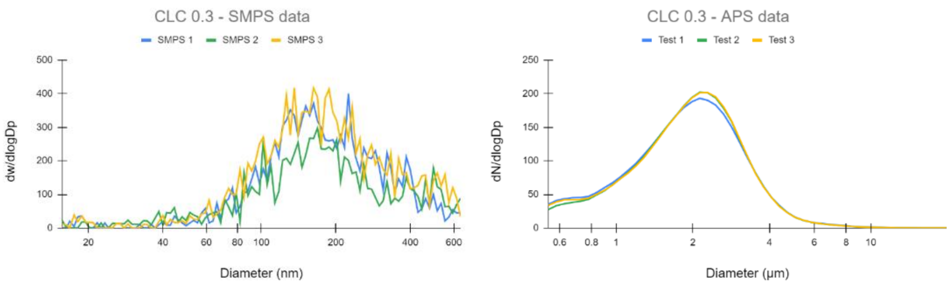

Figure 4.4 Bimodal size distribution of the cellular lightweight concrete with 0.3 wt% carbon nanotubes.

The SMPS size distribution contains higher noise levels than the APS size distribution due to a lower time resolution and fewer data points.

The second pattern showed trimodal distributions for the UHPC, where two modes can be seen, in Figure 4.5, from the SMPS data for the UHPC without CNTs. The APS size distributions showed a similar behaviour as in Figure 4.4 above, with one mode. The trimodal distributions for UHPC show two peaks in the same range as the previous bimodal distribution, with one additional peak at around 500 nm in diameter.

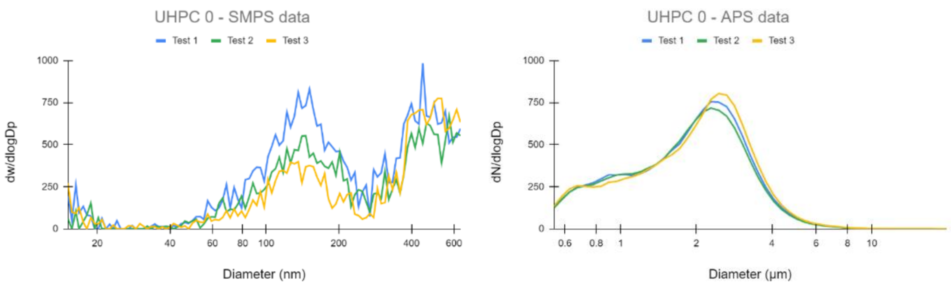

Figure 4.5 Trimodal size distribution of the ultra-high performance concrete without carbon nanotubes.

The third pattern was observed for two of the samples, the NSC with 0.1 wt% CNTs and the CLC without CNTs, and showed a different bimodal size distribution. Figure 4.6 shows the SMPS and APS size distributions for the CLC without CNTs and it shows a peak at around 600 nm and some irregular peaks at diameters smaller than 20 nm. The APS size distributions showed a similar behaviour as above, with one mode.

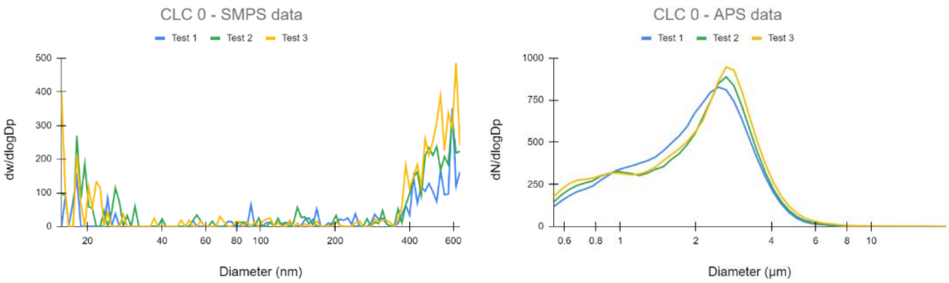

Figure 4.6 Size distributions of the cellular lightweight concrete without carbon nanotubes.

All the peak diameters in the measured size range were smaller than 4 µm, the upper limit for the respirable fraction.

4.2.2 **Number concentrations**

The number concentrations were measured with the APS, CPC and NanoTracer. The APS and CPC showed stable concentration levels during the sampling time, while the measured NanoTracer concentrations were more fluctuating.

The number concentration levels stabilized after 2-3 minutes and some of the tests showed peaks at the start, see Figure 4.7, indicating that it takes some time for the dust generation to stabilize. The most prominent peaks were visible in the graphs from the CPC data, which measures particles ranging 7 - 2 000 nm in diameter.

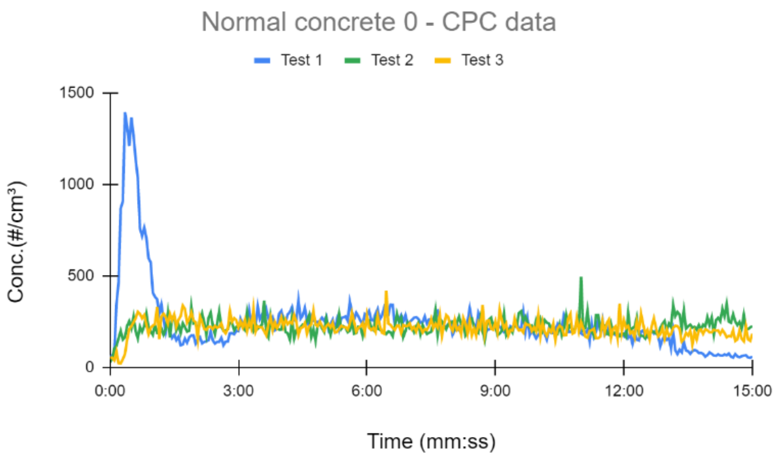

Figure 4.7 Number concentrations from the CPC data for the normal strength concrete without carbon nanotubes. Test 1 shows a peak at the start of the test.

Figure 4.8 shows concentration levels from the APS of the UHPC without CNTs, without any transient peaks at the start. The concentration levels stabilize after three minutes.

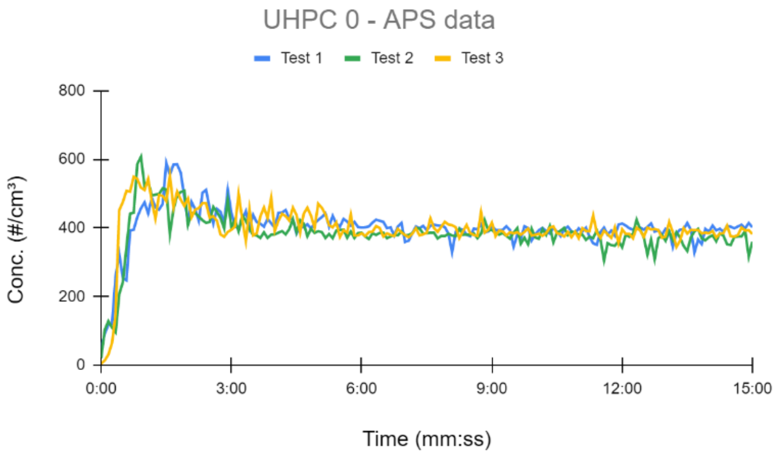

Figure 4.8 Number concentrations from the APS data for the ultra-high performance concrete without carbon nanotubes.

Figure 4.9 shows the NanoTracer concentrations for the same sample, UHPC without CNTs. The concentrations from the NanoTracer vary more between tests than the concentration levels from the APS, in Figure 4.8. The NanoTracer measures particles in another size range and has a lower time resolution than the APS instrument, see Table 3.2.

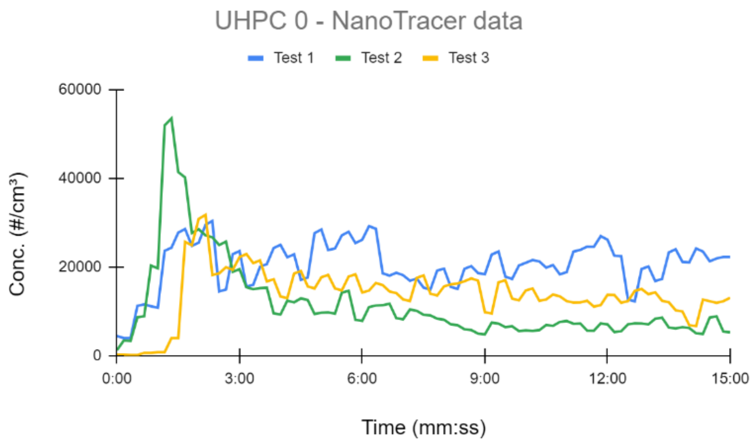

Figure 4.9 Number concentrations from the NanoTracer for the ultra-high performance concrete without carbon nanotubes.

4.2.3 Mass concentrations

The mass concentrations were measured directly with the DustTrak (in the respirable fraction) as well as calculated from the gravimetric filter samples (for both the total fraction and the respirable fraction). The concentration levels from the DustTrak (see Appendix A and C) and the respirable gravimetric results differ from each other by different factors, see Table 4.2. Since the DustTrak assesses mass concentrations based on an optical method, the results need to be adjusted according to the respirable gravimetric measurements. The calculated mass concentrations are listed in Appendix B.

Table 4.2 DustTrak and Gravimetric average mass concentrations.

Sample type	DustTrak average (mg/m^3)	Gravimetric average (mg/m^3)	Fraction DT/Gravimetric
NSC 0	4.4	3.0	1.47
NSC 0.05	5.5	4.1	1.34
NSC 0.1	-	6.7	-
CLC 0	24.1	11.3	2.13
CLC 0.1	10.6	3.3	3.21
CLC 0.3	9.45	4.1	2.30
UHPC 0	8.1	7.2	1.13
UHPC 0.3	6.2	4.4	1.41
UHPC 0.5	8.6	7.7	1.12

The difference was highest for the CLC, where the measured DT were 2-3 times higher than the gravimetric results, while the DT mass concentrations were approximately 12-47 % higher for the NSC and UHPC. Due to the measuring techniques, the gravimetric results are the most reliable.

The gravimetric results show a large variation in mass concentrations for the total dust fraction. For example, the UHPC with 0.5 wt% CNTs varied from 40 mg/m^3 to 330 mg/m^3 which is a factor of approximately 8. The test-to-test variations were smaller for the respirable fraction, with calculated average values ranging from approximately 3 to 11 mg/m^3.

4.2.4 SEM images

The filters for SEM analysis were used for visual analysis to see if there are any free CNTs in the generated dust or if the CNTs seem to be bound to the concrete matrix particles.

Figure 4.10 shows a concrete particle from the UHPC with 0.5 wt% CNTs.

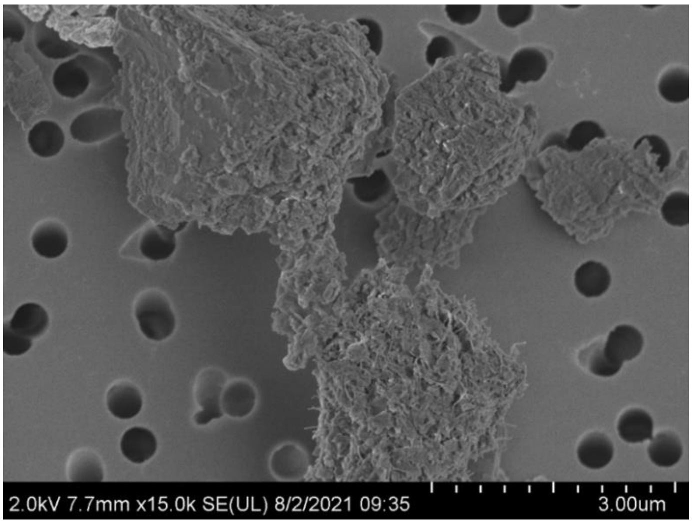

Figure 4.10 SEM image of concrete particle with carbon nanotubes. From the ultra-high performance concrete with 0.5 wt% carbon nanotubes.

Figure 4.11 shows a close-up of the same particle with the carbon nanotubes protruding from the concrete matrix.

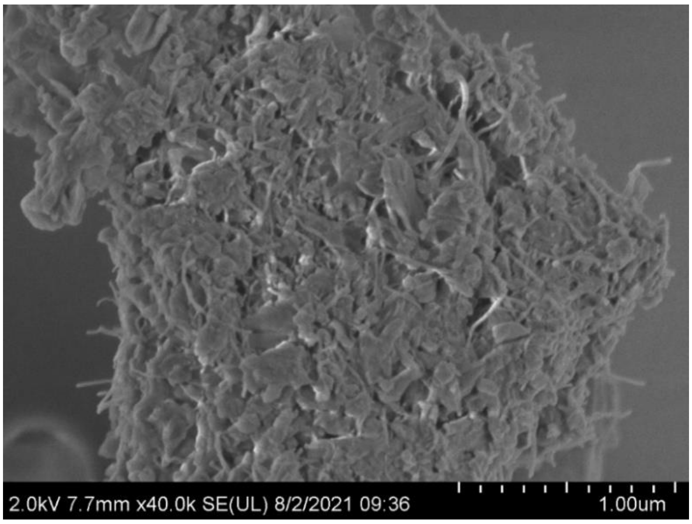

Figure 4.11 Close-up of a concrete particle from the ultra-high performance concrete with 0.5 wt% carbon nanotubes.

For comparison, Figure 4.12 shows a particle from the UHPC without any carbon nanotubes. The fiber-shaped particles protruding from the particle are no longer present. More SEM-images from the other samples are shown in Appendix D.

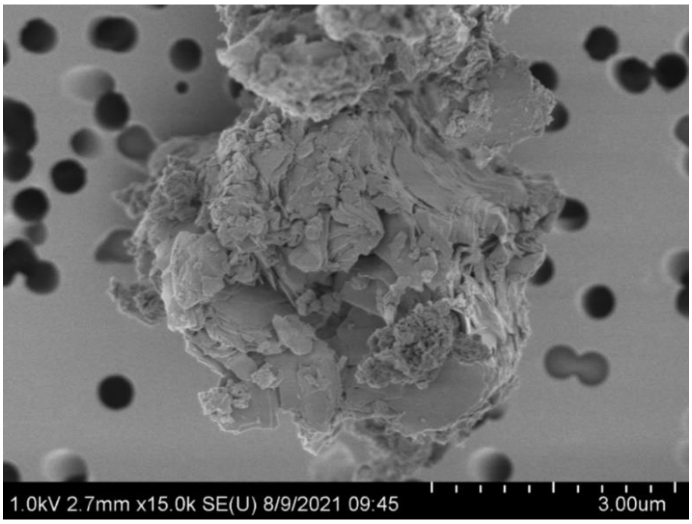

Figure 4.12 Concrete particle from the ultra-high performance concrete without carbon nanotubes.

5 Discussion

The three tests per sample type were similar in the average concentrations, which indicates reproducibility, as can be seen in Figures 4.1 to 4.3. Some tests showed peaks in the concentration at the start. For example, the peak in Test 1 in Figure 4.7 is visible in the CPC data but not the APS or DustTrak data. Since the CPC detects smaller particles (7 – 2000 nm) than the APS (500 – 20 000 nm), the peak can be assumed to be caused by smaller particles. Small particles do not generally contribute much to mass concentrations, which is likely to be the reason that the peak is not visible in the DustTrak measurements. This is also consistent with the size distribution data from the SMPS and APS, since the SMPS shows a higher concentration for Test 1. The peaks were present in some of the tests of the NSC and UHPC, but most of the tests did not include a peak at the start. Therefore, this peak can be assumed to be a result from the dust generation method, rather than a property of the concrete. After the initial peak the concentration level stabilized at the same level as in the other tests. This means that the tests can be assumed to be equivalent after the initial transient processes. This also motivates a delayed start of the filter sampling. The filter sampling was started two minutes after the start of the experiment, but based on these results three minutes would be a better delay.

The drop mass flow was roughly ten times lower in these experiments compared to the specifications in the EN 15051-3 standard. This lower drop mass flow was accepted in order to obtain stable concentration levels during the entire testing time. Since the dustiness classifications in the standard were based on the fraction between the aerosolized material and the fallen material, they could still be calculated from these experiments. This made it possible to compare the dustiness of the concrete types relative one another. From the results of the experiments with the sifted crushed concrete, all concrete types were of “moderate” dustiness, which is the second highest category of four dustiness categories described in the EN 15051-3 standard. The material that was sifted away would in theory not be aerosolized due to the particle sizes and therefore it would contribute more to the fallen and collected mass. By compensating the calculated respirable dustiness mass fractions with the total amount of material, a lower dustiness level was achieved. These results showed that the CLC was the concrete type with the highest dustiness levels, even though the UHPC showed the highest number particle concentrations from the online instruments.

The results show for all concrete types that the dustiness first decreases and then increases with the addition of CNTs. However, the NSC and UHPC has the highest dustiness with the highest concentration of CNTs, while the CLC has the highest dustiness without CNTs. This indicates a non-linear relationship between the concentration of CNTs and the dustiness of the concrete. To draw any further conclusions, more testing on more CNT concentrations would be needed.

Based on the results of this study, the presence of CNTs affect the different concrete types differently and different concentrations of CNTs can either increase or decrease the dustiness, which means that each concrete type needs to be classified individually regarding dustiness. They also indicate that lightweight and porous concretes produce higher dustiness levels than concretes with higher densities.

The high dustiness level of the CLC was also seen during the crushing process as most of the crushed CLC particles (88-97 %) were smaller than 0.850 mm, the sifting size limit, while a lower fraction (around 30-40 %) of the NSC and UHPC was smaller than 0.850 mm. The CLC was easily crushed and could be crushed by hand, which could have an impact on the dustiness as new particles were more easily formed.

The dustiness categories are based on dustiness testing of powder bulk materials, where the powder particles are likely more uniform in size. The crushed concrete is not strictly a powder material and the particle size distribution depends on the crushing process. Therefore, the measured dustiness categories may not be representative as absolute values of dustiness of the different concretes in bulk. It is also important to keep in mind that the continuous drop method does not take all properties that affect dustiness into account. For instance, it is not applicable for evaluating processes where solid concrete is being treated mechanically, such as drilling or polishing. However, it is still useful to keep in mind that the CLC has a higher propensity for releasing dust and this property can be relevant when handling the concrete in other dust-generating processes.

All the size distributions from these experiments have peak diameters below 4 µm, which is the upper limit for the respirable fraction. This further motivates toxicity studies of concrete particles containing engineered nanoparticles, since they are likely to reach the alveolar region of the human respiratory system.

The SMPS data showed significant differences in the size distributions, with three main patterns in the nanometer-size range (as described in chapter 4.2.1). All the distributions had similar modes in the APS data, with one mode at around 2 µm. Therefore, in order to fully investigate the particle size distribution it is important to include measurements that cover the entire area of interest, as has been done in this study.

The gravimetric results show a large variation in mass concentrations for the total dust fraction, which can be attributed to larger particles that drastically change the filter mass. However, the respirable filters show a smaller degree of variation, as the larger particles were separated by a PM4 cyclone. The respirable fraction is the most interesting result regarding health effects since it is the fraction that reaches the deepest in the respiratory airways (CEN, 1993). Occupational exposure limit values are often defined from the mass concentrations and the Occupational Safety and Health Administration (OSHA) has recommendations of permissible exposure limits at 5 mg/m^3 for respirable dust and 15 mg/m^3 for total dust fractions (OSHA, 2018). The mass concentration measurements in this study show that both the total fraction and respirable fraction are higher than the permissible exposure limits, see Appendix B.

Other previous studies related to workplace exposures of concrete dust in the construction industry have focused on silica exposure. One study from 1988 (Riala, 1988) investigated the dust concentrations associated with cleaning at construction sites, activities that are within the scope of the continuous drop-method. Dry sweeping of concrete dust yielded the highest concentrations up to 117 mg/m^3 (with a mean concentration of 32 mg/m^3) in the total fraction and up to 1.9 mg/m^3 (with a mean concentration of 0.53 mg/m^3) in the respirable fraction. Another study from 2014 (Kohlman-Rabbani, 2014) investigated the inhalable and respirable dust concentrations from dust-generating activities at construction sites. Activities that fall under the scope of the continuous drop-method such as concrete mixing and cleaning yielded mass concentrations of 2.7 mg/m^3 for the total fraction and 0.5 mg/m^3 for the respirable fraction. These measured mass concentrations are lower than the measured concentrations from this project, but these two studies show that there is a large variation depending on the dust generating process at different workplace environments.

The air exchange rate in the main cylinder was around 2.7 times per minute which is high compared to regular levels for indoor office environments that are usually in the order of 2-3 per hour. (ASHRAE, 2016). The air velocities at construction sites are likely to be higher, but not at the level of 2.7 times per minute. The continuous drop method in this study is a laboratory setup and generates higher aerosol concentrations than actual workplace measurements. It is useful for comparing the dustiness between different concrete materials and needs to be combined with workplace measurements in order to fully assess the occupational risks.

The SEM images show some morphological differences between the particles with and without CNTs. The CNTs are visible in the concrete matrix, but it is difficult to determine how embedded they are in the concrete or if they are loosely bound to the surface of the concrete particles. It is not possible to exclude the presence of single CNTs or pure agglomerates of CNTs. Previous SEM-studies of airborne CNTs have shown that they often occur as agglomerates. One study from 2015 (Kujipers, 2015) on the occupational exposures from MWCNTs during production and handling showed that the CNTs predominantly existed in agglomerates, with peak diameters in the range of 0.65-1 µm.

If the CNTs in the aerosol particles mainly occur embedded in the concrete, it is possible that this affects the toxicity as the fiber properties are mitigated. However, it is still unknown how the CNT-containing concrete particles behave after deposition in the respiratory system. If the CNTs disperse, the fiber properties are still relevant and a possible health hazard.

The DustTrak and NanoTracer instruments are cheaper and portable and can be used as handheld instruments for exposure monitoring at workplaces. The measured concentration levels were high in noise and the test-to-test variation was higher compared to the other online instruments, see Appendix A. However, these instruments are still useful in order to detect short-term variations or long-term increasing trends in particle concentrations. To determine accurate concentration levels the measured DustTrak results need to be adjusted with gravimetric filter measurements, as seen in Table 4.2.

There were some deviations from the EN 15051 standard. According to the standard the density and humidity of the dust were supposed to be measured before testing, but in these experiments the concrete samples were conditioned in the exposure chamber for at least 24 hours before testing in order to ensure similar temperature and humidity. The relative humidity and temperature in the exposure chamber were adjusted to a lower level than the defined levels in the standard, to the capacity of the equipment controlling the exposure chamber. In addition, there was a limited supply of material and there was not enough material to start every test with 100 g, as was first intended. However, since not all the material fell from the top container during the measurement time this was assumed to not have a significant impact on the measured concentrations.

6 Conclusions

This project shows that the concrete dustiness is affected differently by the presence of carbon nanotubes for different types of concrete and that the concentration of carbon nanotubes can either increase or decrease the dustiness depending on the concentration.

For the CLC the dustiness was highest without carbon nanotubes, while the NSC and UHPC had the highest dustiness levels for the concrete with the highest concentration of carbon nanotubes. All the concrete types had the lowest dustiness for the concrete with the lowest concentration of added carbon nanotubes.

According to the dustiness categories from the EN 15051-3 standard, the CLC was the concrete with the highest dustiness (all three types were “moderate”), the UHPC was the second highest (two “moderate” types and one “low”) and the NSC was the lowest (one “moderate” and two “low”).

The continuous drop-setup produced reproducible results in between replicates, but improvements could be made with a higher drop mass flow and a cleaner process to weigh collected material after experiments.

The SEM images show carbon nanotubes embedded in the concrete matrix in the sampled airborne particles, but it is still possible that carbon nanotubes appear in the aerosol as either free fibers or agglomerates.

All peak diameters in the number size distributions are in the respirable fraction, which further motivates toxicity studies of CNT-containing concrete particles.

DustTrak measurements for determining occupational exposures of this type of concrete dust should be performed with caution unless the data can be calibrated with gravimetric filter sampling.

6.1 Outlook

It would be of interest to further investigate why the presence of carbon nanotubes affects different concrete types differently. It would also be relevant to further assess if the CNTs in the dust are free or if they are part of the concrete matrix, as well as if the CNTs are present to a higher degree in some airborne fractions than other.

The attempt for quantifying the carbon nanotubes in the aerosol particles generated by the continuous drop and compare it to the crushed concrete bulk was prepared for, by sampling particles with a PM4 cyclone on quartz filters for OC/EC analysis. It is not yet completely established whether the OC/EC will work for this purpose, since the carbon nanotubes might not be effectively removed by the heating process if they are embedded in the concrete.

In order to further understand the effects of dustiness from the presence of carbon nanotubes, more CNT concentrations could be tested.

The continuous drop setup was built according to the EN 15051-3 standard, but some aspects could be improved such as increasing the drop mass flow to the levels defined in the standard and decreasing the amounts of spill from the collecting and weighing step of the crushed concrete after experiments. It is also recommended to look further into the effects from the relative humidity and temperature.

In order to further understand the health hazards associated with CNT-enhanced concrete, both toxicity studies and workplace measurements need to be carried out as well as study particle emissions from other dust generating processes, such as drilling or crushing of concrete.

References

ASHRAE. 2016. ANSI/ASHRAE Standard 62.1-2016, Ventilation for Acceptable Indoor Air Quality. Atlanta: ASHRAE

Baloch, W. L., Khushnood, R. A., & Khaliq, W. (2018). Influence of multi-walled carbon nanotubes on the residual performance of concrete exposed to high temperatures. Construction and Building Materials, 185, 44-56.

Brown, J.S., Gordon, T., Price, O. and Asgharian, B., 2013. Thoracic and respirable particle definitions for human health risk assessment. Particle and fibre toxicology, 10(1), pp.1-12.

Chan, L. Y., & Andrawes, B. (2010). Finite element analysis of carbon nanotube/cement composite with degraded bond strength. Computational Materials Science, 47(4), 994-1004.

Dai, H. (2002). Carbon nanotubes: opportunities and challenges. Surface Science, 500(1-3), 218-241.

Donaldson, K., Aitken, R., Tran, L., Stone, V., Duffin, R., Forrest, G., & Alexander, A. (2006). Carbon nanotubes: a review of their properties in relation to pulmonary toxicology and workplace safety. Toxicological sciences, 92(1), 5-22.

Donaldson, K., Murphy, F. A., Duffin, R., & Poland, C. A. (2010). Asbestos, carbon nanotubes and the pleural mesothelium: a review of the hypothesis regarding the role of long fibre retention in the parietal pleura, inflammation and mesothelioma. Particle and fibre toxicology, 7(1), 1-17.

Ellenbecker, M., Tsai, S. J., Jacobs, M., Riediker, M., Peters, T., Liou, S., ... & FossHansen, S. (2018). The difficulties in establishing an occupational exposure limit for carbon nanotubes. Journal of Nanoparticle Research, 20(5), 1-12.

European Committee for Standardization (CEN) Workplace atmospheres-size fraction definitions for measurement of airborne particles (Report No. BS EN 481:1993) London, England: CEN, British Standards Institute; 1993.

Gupta, T. K., & Kumar, S. (2018). Fabrication of carbon nanotube/polymer nanocomposites. In Carbon Nanotube-Reinforced Polymers (pp. 61-81). Elsevier.

Hu, Y., Luo, D., Li, P., Li, Q., & Sun, G. (2014). Fracture toughness enhancement of cement paste with multi-walled carbon nanotubes. Construction and Building Materials, 70, 332-338.

Klippel, A., Schmidt, M., & Krause, U. (2015). Dustiness in workplace safety and explosion protection–review and outlook. Journal of loss prevention in the process industries, 34, 22-29.

Kohlman-Rabbani, E. R., Shapira, A., Martins, A. R. B., & Barkokébas Jr, B. (2014). Characterization and evaluation of dust on building construction sites in brazil. The Open Occupational Health & Safety Journal, 5(1).

Konsta-Gdoutos, M. S., Metaxa, Z. S., & Shah, S. P. (2010). Multi-scale mechanical and fracture characteristics and early-age strain capacity of high performance carbon nanotube/cement nanocomposites. Cement and Concrete Composites, 32(2), 110-115.

Kuijpers, E., Bekker, C., Fransman, W., Brouwer, D., Tromp, P., Vlaanderen, J., ... & Pronk, A. (2016). Occupational exposure to multi-walled carbon nanotubes during commercial production synthesis and handling. Annals of occupational hygiene, 60(3), 305-317.

Kulkarni, P., Baron, P. A., & Willeke, K. (Eds.). (2011). Aerosol measurement: principles, techniques, and applications. John Wiley & Sons.

Lidén, G. (2006). Dustiness testing of materials handled at workplaces. The Annals of occupational hygiene, 50(5), 437-439.

Lim, M. J., Lee, H. K., Nam, I. W., & Kim, H. K. (2017). Carbon nanotube/cement composites for crack monitoring of concrete structures. Composite Structures, 180, 741-750.

Lu, L., Ouyang, D., & Xu, W. (2016). Mechanical properties and durability of ultra high strength concrete incorporating multi-walled carbon nanotubes. Materials, 9(6), 419.

Löndahl, J., Möller, W., Pagels, J. H., Kreyling, W. G., Swietlicki, E., & Schmid, O. (2014). Measurement techniques for respiratory tract deposition of airborne nanoparticles: a critical review. Journal of aerosol medicine and pulmonary drug delivery, 27(4), 229–254. https://doi.org/10.1089/jamp.2013.1044

Marra, J., Voetz, M., & Kiesling, H. J. (2010). Monitor for detecting and assessing exposure to airborne nanoparticles. Journal of Nanoparticle Research, 12(1), 21-37.

Modena, M. M., Rühle, B., Burg, T. P., & Wuttke, S. (2019). Nanoparticle characterization: what to measure?. Advanced Materials, 31(32), 1901556.

Nanocyl, NC7000™. (n.d.). Retrieved April 20th 2021, from https://www.nanocyl.com/product/nc7000/

OSHA, Flavorings-Related Lung Disease: Occupational Exposure Limits. (2018). Retrieved August 7th 2021 from https://www.cdc.gov/niosh/topics/flavorings/limits.html

Popov, V. N. (2004). Carbon nanotubes: properties and application. Materials Science and Engineering: R: Reports, 43(3), 61-102.

Riala, R. (1988). Dust and quartz exposure of Finnish construction site cleaners. The Annals of occupational hygiene, 32(2), 215-220.

RISE. Cellular lightweight concrete. (n.d.). Retrieved August 3rd 2021, from https://www.ri.se/en/what-we-do/expertises/cellular-lightweight-concrete

RISE. Ultra-high Performance Concrete. (n.d.). Retrieved August 3rd 2021, from https://www.ri.se/en/what-we-do/expertises/uhpc

Sanchez, V. C., Pietruska, J. R., Miselis, N. R., Hurt, R. H., & Kane, A. B. (2009). Biopersistence and potential adverse health impacts of fibrous nanomaterials: what have we learned from asbestos?. Wiley Interdisciplinary Reviews: Nanomedicine and Nanobiotechnology, 1(5), 511-529.

Seipenbusch, M., Binder, A., & Kasper, G. (2008). Temporal evolution of nanoparticle aerosols in workplace exposure. Annals of occupational hygiene, 52(8), 707-716.

Thostenson, E. T., Ren, Z., & Chou, T. W. (2001). Advances in the science and technology of carbon nanotubes and their composites: a review. Composites science and technology, 61(13), 1899-1912.

Viitanen, A. K., Uuksulainen, S., Koivisto, A. J., Hämeri, K., & Kauppinen, T. (2017). Workplace measurements of ultrafine particles—a literature review. Annals of Work Exposures and Health, 61(7), 749-758.

Xu, S., Liu, J., & Li, Q. (2015). Mechanical properties and microstructure of multi-walled carbon nanotube-reinforced cement paste. Construction and Building Materials, 76, 16-23.

Yakovlev, G., Kerienė, J., Gailius, A., & Girnienė, I. (2006). Cement based foam concrete reinforced by carbon nanotubes. Materials Science [Medžiagotyra], 12(2), 147-151.

Yang, H. Q., Yu, H. S., & Zhao, X. (2014). Reinforcement of the mechanical and durability performance of cement-based materials with multi-walled carbon nanotubes. Journal of Advanced Microscopy Research, 9(2), 93-96.

Zhou, W., Apkarian, R., Wang, Z. L., & Joy, D. (2006). Fundamentals of scanning electron microscopy (SEM). In Scanning microscopy for nanotechnology (pp. 1-40). Springer, New York, NY.

Appendix A

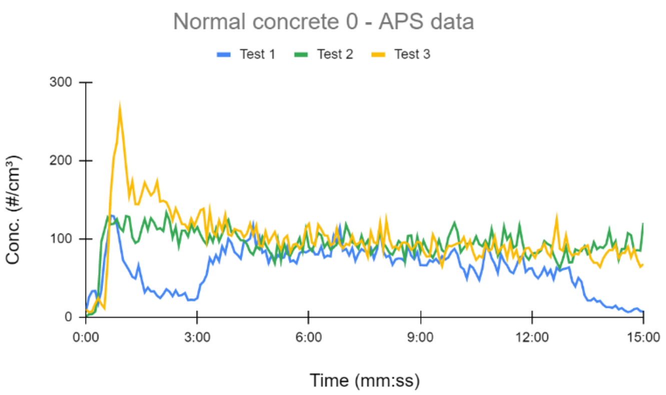

Normal concrete 0 - APS data
Test 1 Test 2 Test 3
Conc. (#/cm³)
Time (mm:ss)

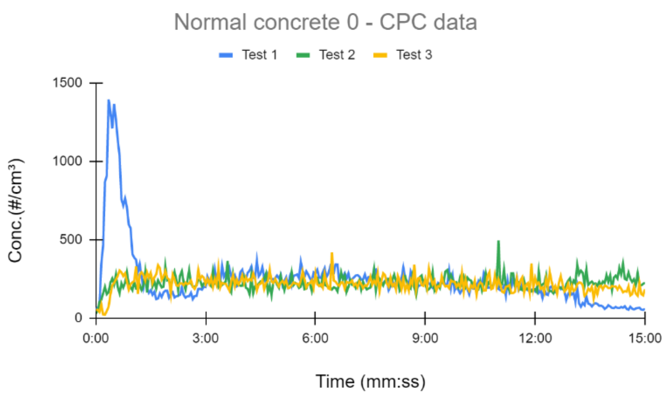

Normal concrete 0 - CPC data
Test 1 Test 2 Test 3
Conc.(#/cm³)
Time (mm:ss)

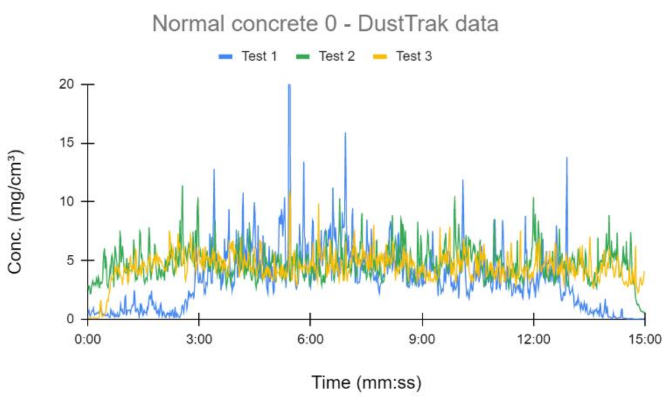

Normal concrete 0 - DustTrak data
Test 1 Test 2 Test 3
Conc. (mg/cm³)
Time (mm:ss)

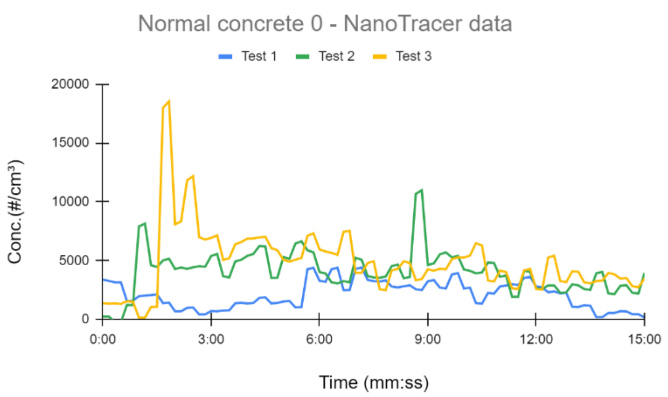

Normal concrete 0 - NanoTracer data
Test 1 Test 2 Test 3
Conc.(#/cm³)
Time (mm:ss)

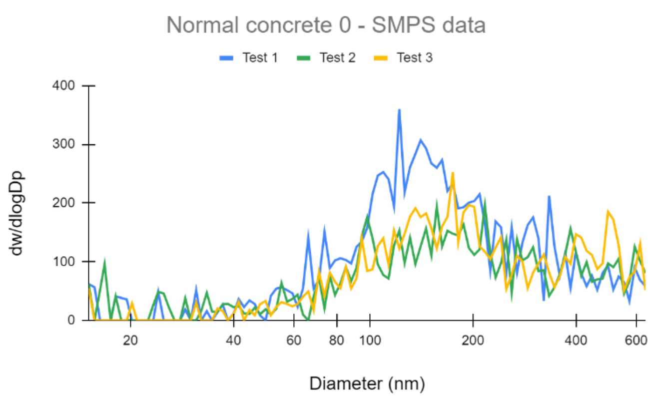

Normal concrete 0 - SMPS data
Test 1 Test 2 Test 3
dw/dlogDp
Diameter (nm)

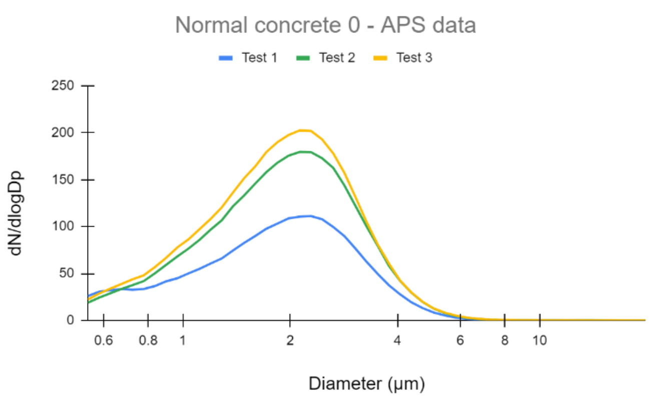

Normal concrete 0 - APS data
Test 1 Test 2 Test 3
dN/dlogDp
Diameter (µm)

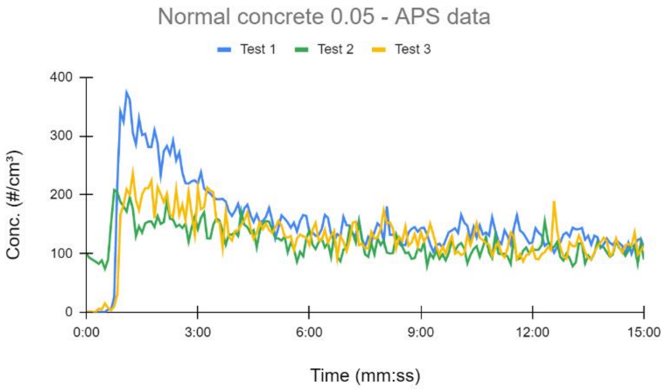
Normal concrete 0.05 - APS data
Test 1
Test 2
Test 3
Conc. (#/cm³)
Time (mm:ss)

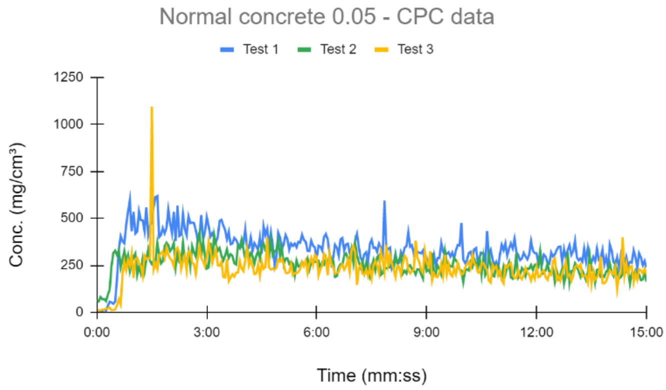
Normal concrete 0.05 - CPC data
Test 1
Test 2
Test 3
Conc. (mg/cm³)
Time (mm:ss)

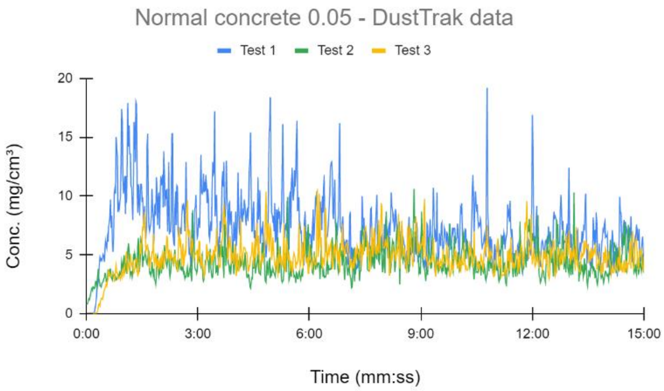
Normal concrete 0.05 - DustTrak data
Test 1
Test 2
Test 3
Conc. (mg/cm³)
Time (mm:ss)

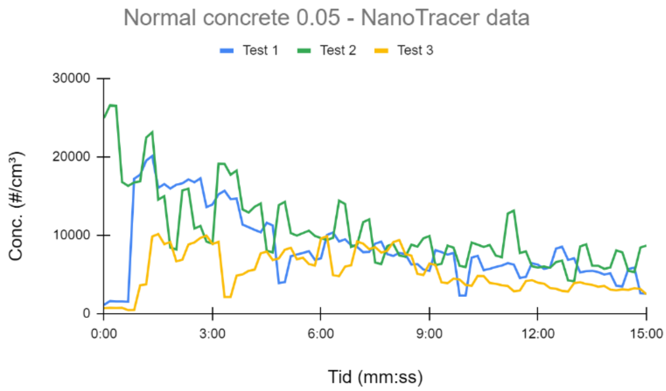
Normal concrete 0.05 - NanoTracer data
Test 1
Test 2
Test 3
Conc. (#/cm³)
Tid (mm:ss)

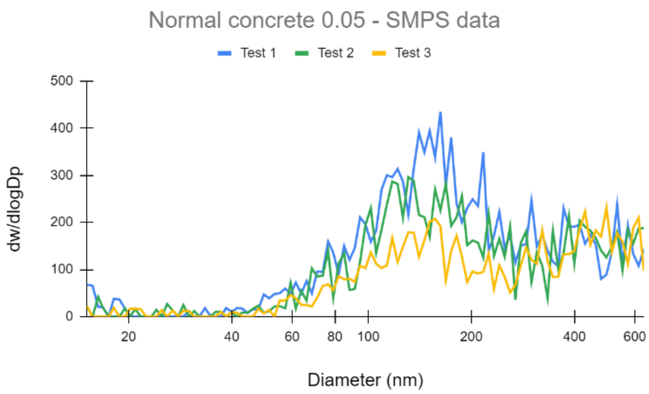
Normal concrete 0.05 - SMPS data
Test 1
Test 2
Test 3
dw/dlogDp
Diameter (nm)

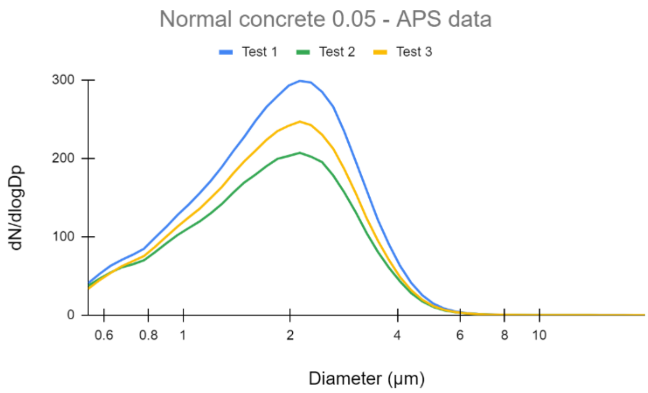
Normal concrete 0.05 - APS data
Test 1
Test 2
Test 3
dN/dlogDp
Diameter (µm)

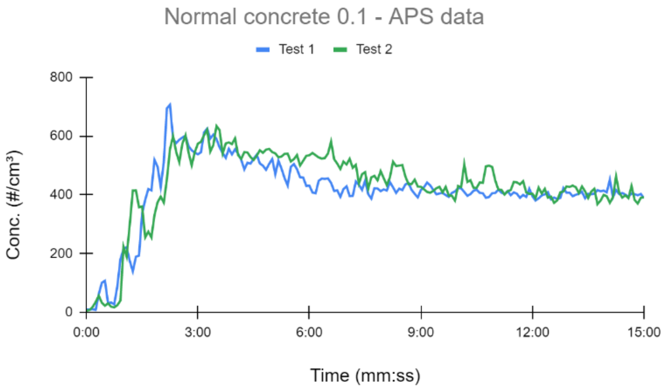

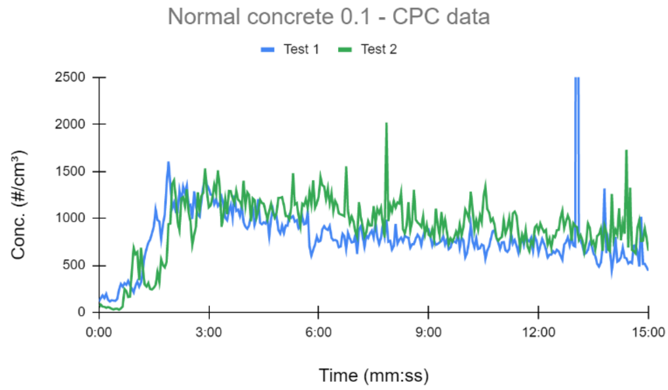

No DustTrak data as the file was corrupted.

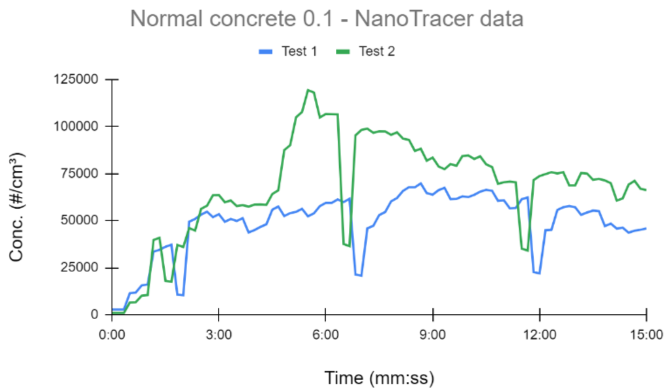

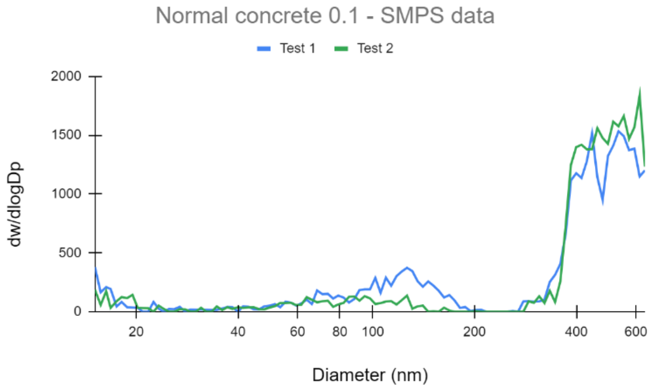

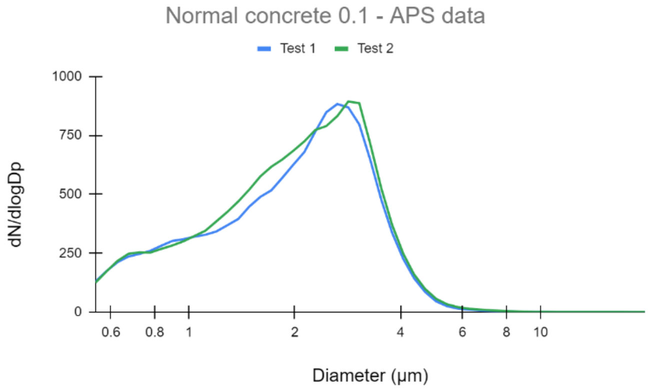

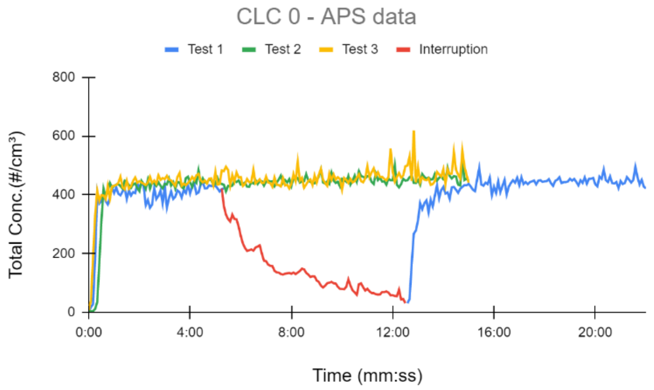
CLC 0 - APS data
Test 1
Test 2
Test 3
Interruption
Total Conc.(#/cm³)
0
200
400
600
800
0:00
4:00
8:00
12:00
16:00
20:00
Time (mm:ss)

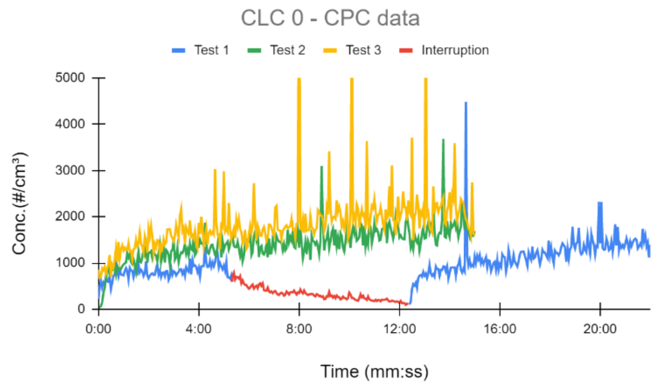
CLC 0 - CPC data
Test 1
Test 2
Test 3
Interruption
Conc.(#/cm³)
0
1000
2000
3000
4000
5000
0:00
4:00
8:00
12:00
16:00
20:00
Time (mm:ss)

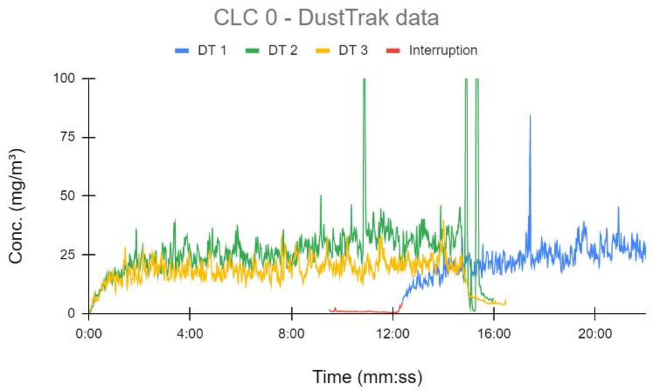
CLC 0 - DustTrak data
DT 1
DT 2
DT 3
Interruption
Conc. (mg/m³)
0
25
50
75
100
0:00
4:00
8:00
12:00
16:00
20:00
Time (mm:ss)

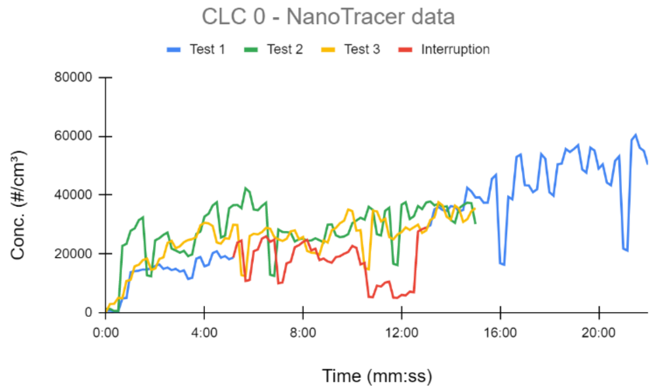
CLC 0 - NanoTracer data
Test 1
Test 2
Test 3
Interruption
Conc. (#/cm³)
0
20000
40000
60000
80000
0:00
4:00
8:00
12:00
16:00
20:00
Time (mm:ss)

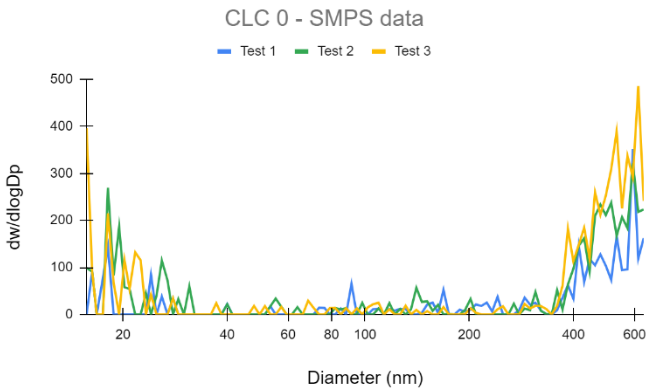
CLC 0 - SMPS data
Test 1
Test 2
Test 3
dw/dlogDp
0
100
200
300
400
500
20
40
60
80
100
200
400
600
Diameter (nm)

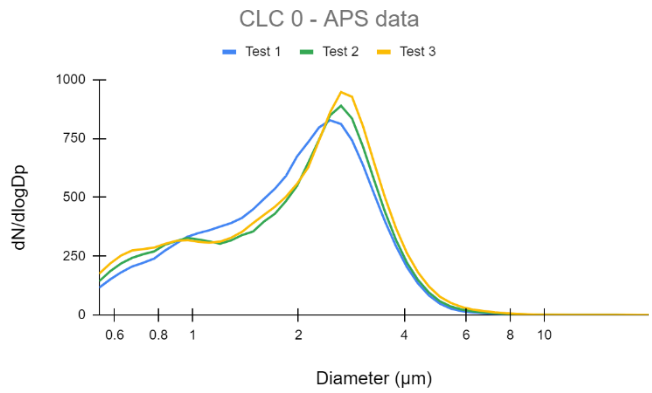
CLC 0 - APS data
Test 1
Test 2
Test 3
dN/dlogDp
0
250
500
750
1000
0.6
0.8
1
2
4
6
8
10
Diameter (µm)

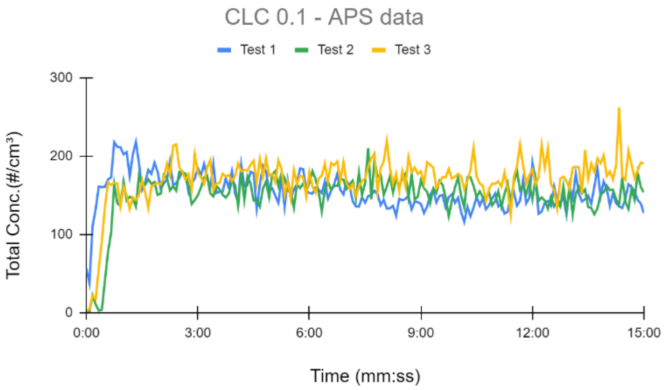
CLC 0.1 - APS data
Test 1
Test 2
Test 3
Total Conc.(#/cm³)
Time (mm:ss)

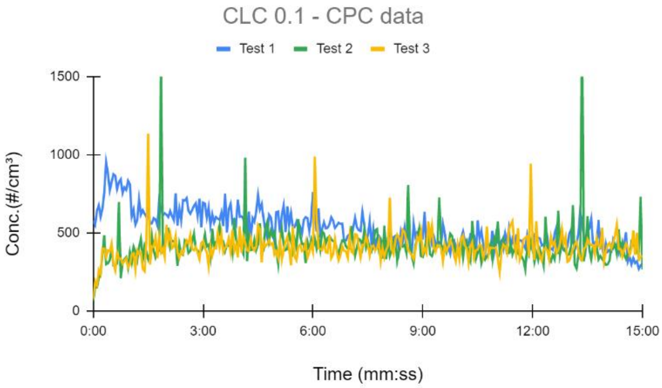
CLC 0.1 - CPC data
Test 1
Test 2
Test 3
Conc.(#/cm³)
Time (mm:ss)

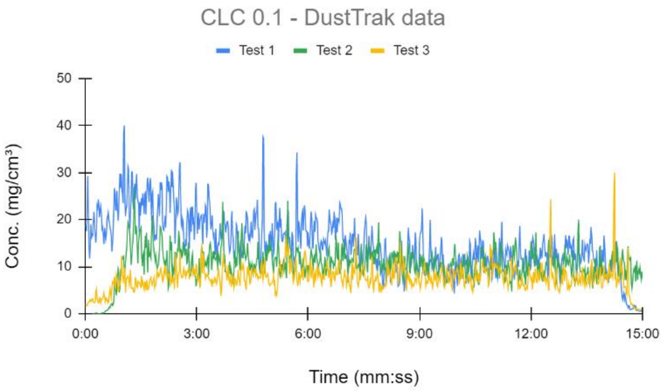
CLC 0.1 - DustTrak data
Test 1
Test 2
Test 3
Conc. (mg/cm³)
Time (mm:ss)

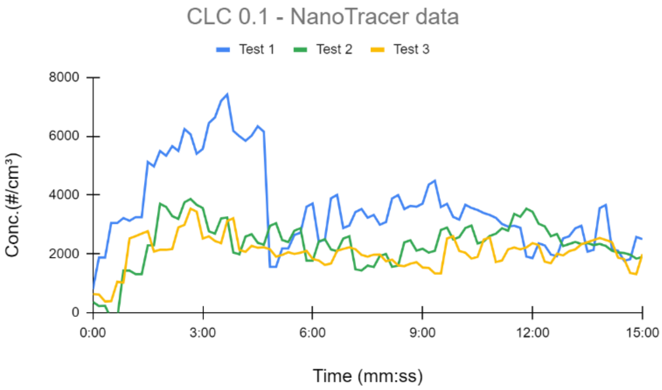
CLC 0.1 - NanoTracer data
Test 1
Test 2
Test 3
Conc.(#/cm³)
Time (mm:ss)

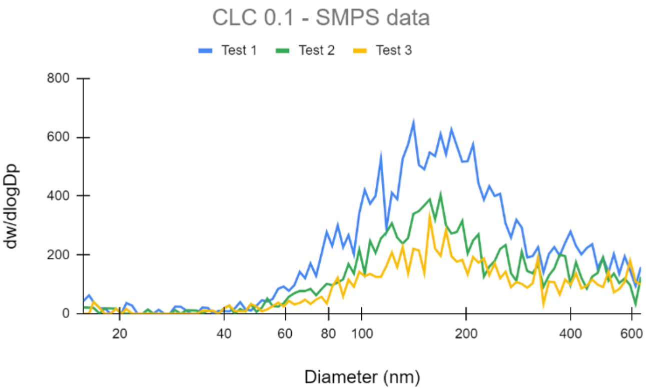
CLC 0.1 - SMPS data
Test 1
Test 2
Test 3
dw/dlogDp
Diameter (nm)

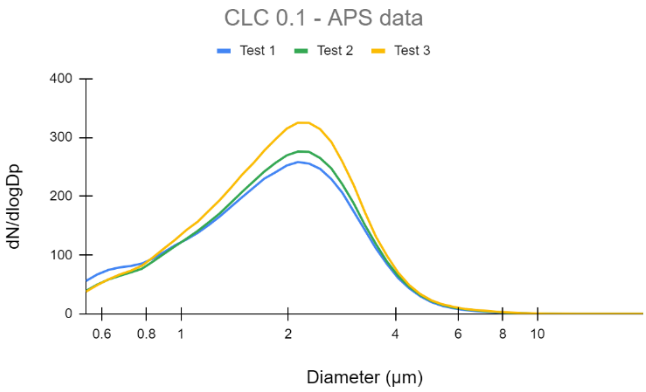
CLC 0.1 - APS data
Test 1
Test 2
Test 3
dN/dlogDp
Diameter (µm)

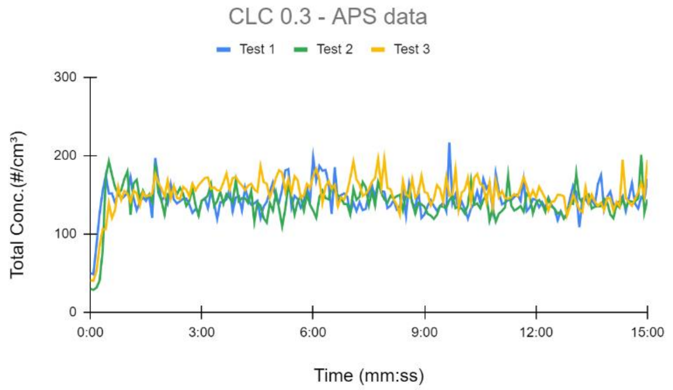
CLC 0.3 - APS data
Test 1
Test 2
Test 3
Total Conc.(#/cm³)
Time (mm:ss)

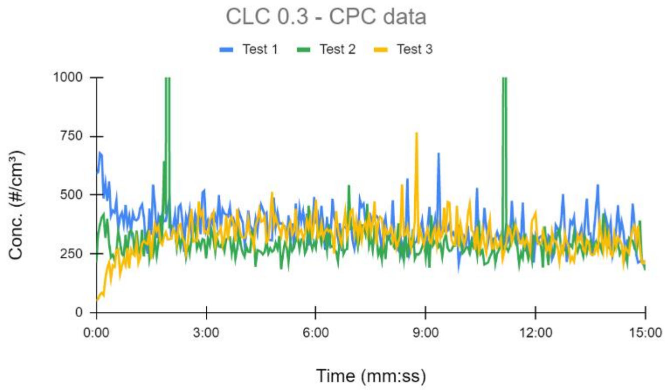
CLC 0.3 - CPC data
Test 1
Test 2
Test 3
Conc. (#/cm³)
Time (mm:ss)

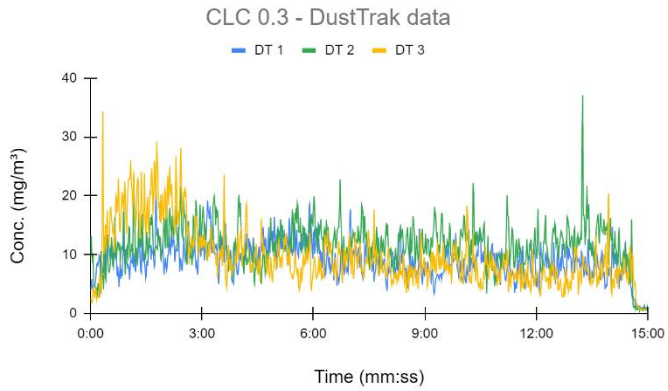
CLC 0.3 - DustTrak data
DT 1
DT 2
DT 3
Conc. (mg/m³)
Time (mm:ss)

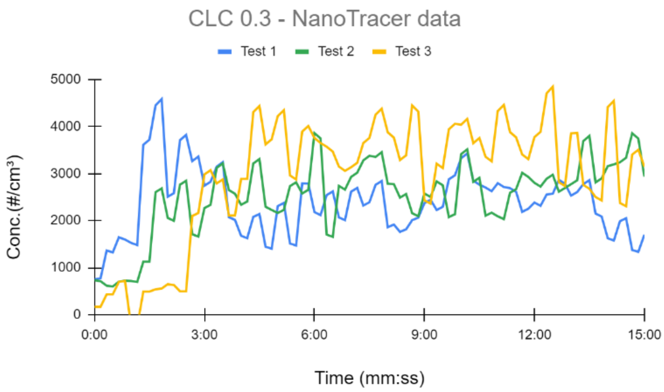
CLC 0.3 - NanoTracer data
Test 1
Test 2
Test 3
Conc.(#/cm³)
Time (mm:ss)

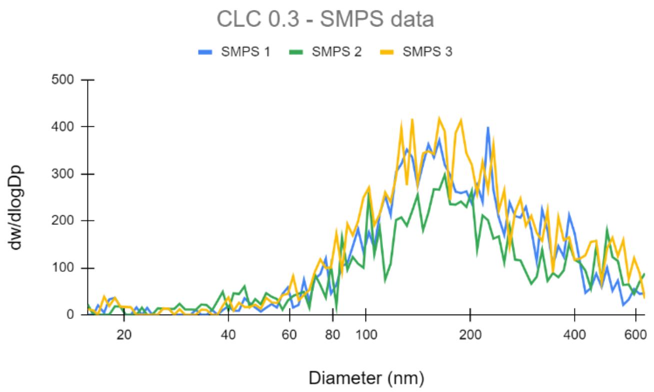
CLC 0.3 - SMPS data
SMPS 1
SMPS 2
SMPS 3
dw/dlogDp
Diameter (nm)

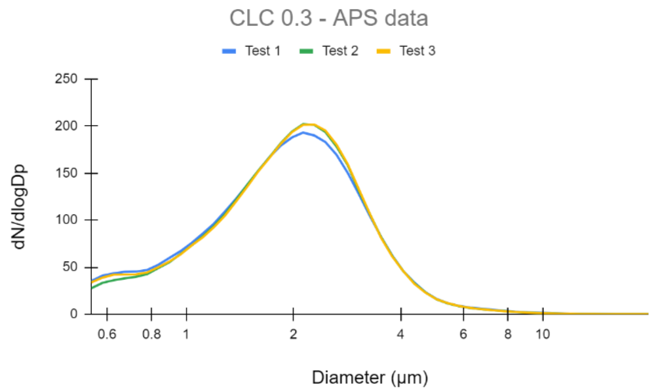
CLC 0.3 - APS data
Test 1
Test 2
Test 3
dN/dlogDp
Diameter (μm)

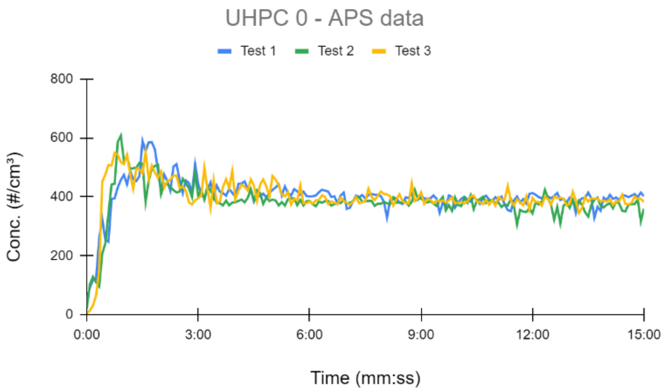
UHPC 0 - APS data
Test 1
Test 2
Test 3
Conc. (#/cm³)
800
600
400
200
0
0:00
3:00
6:00
9:00
12:00
15:00
Time (mm:ss)

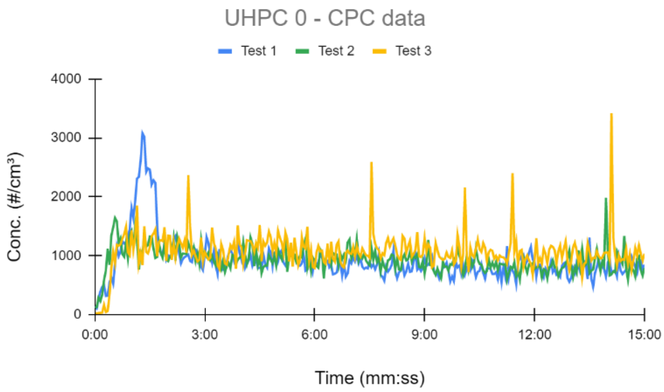
UHPC 0 - CPC data
Test 1
Test 2
Test 3
Conc. (#/cm³)
4000
3000
2000
1000
0
0:00
3:00
6:00
9:00
12:00
15:00
Time (mm:ss)

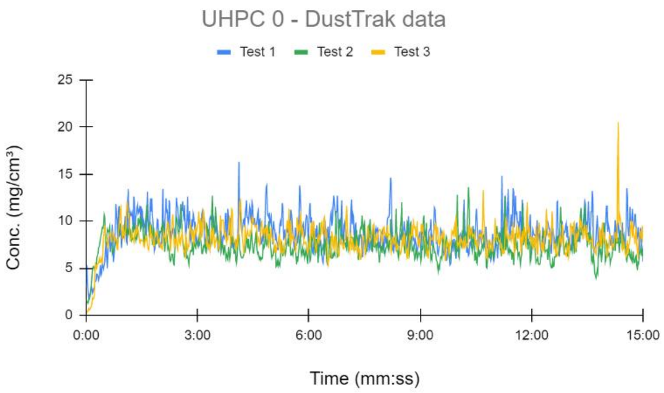
UHPC 0 - DustTrak data
Test 1
Test 2
Test 3
Conc. (mg/cm³)
25
20
15
10
5
0
0:00
3:00
6:00
9:00
12:00
15:00
Time (mm:ss)

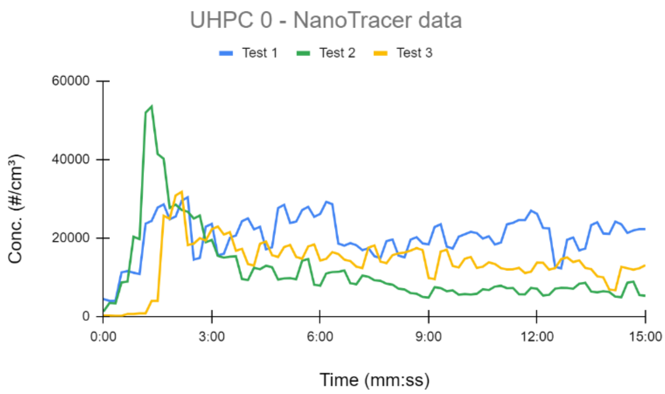
UHPC 0 - NanoTracer data
Test 1
Test 2
Test 3
Conc. (#/cm³)
60000
40000
20000
0
0:00
3:00
6:00
9:00
12:00
15:00
Time (mm:ss)

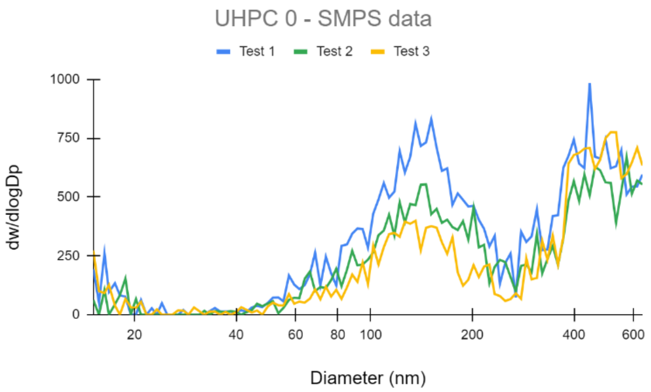
UHPC 0 - SMPS data
Test 1
Test 2
Test 3
dw/dlogDp
1000
750
500
250
0
20
40
60
80
100
200
400
600
Diameter (nm)

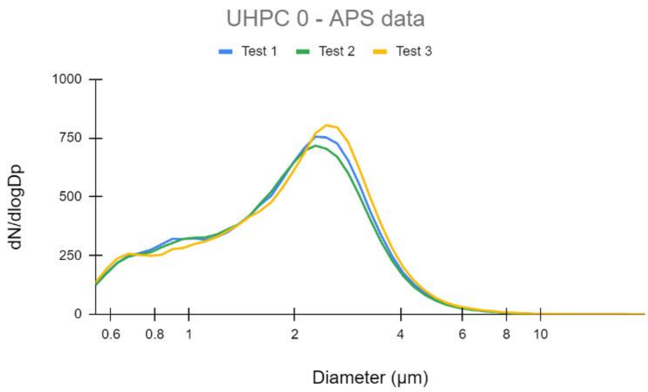
UHPC 0 - APS data
Test 1
Test 2
Test 3
dN/dlogDp
1000
750
500
250
0
0.6
0.8
1
2
4
6
8
10
Diameter (µm)

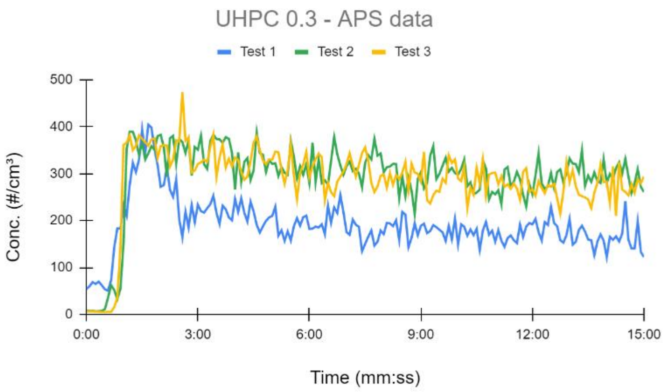
UHPC 0.3 - APS data
Test 1
Test 2
Test 3
Conc. (#/cm³)
Time (mm:ss)

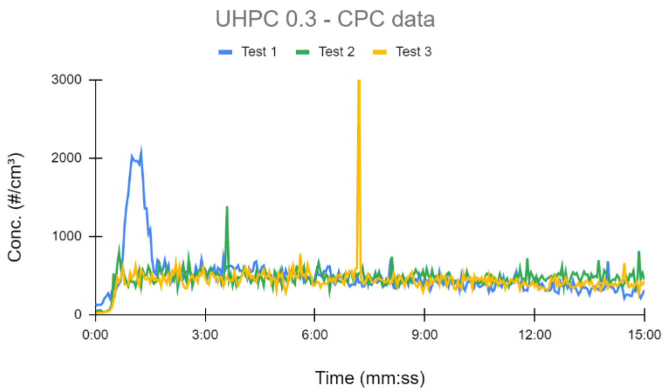
UHPC 0.3 - CPC data
Test 1
Test 2
Test 3
Conc. (#/cm³)
Time (mm:ss)

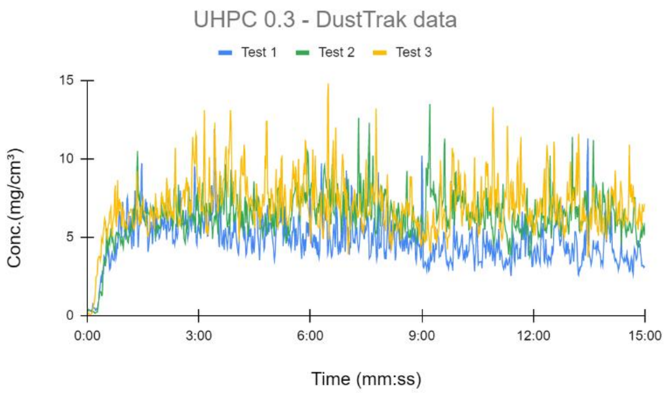
UHPC 0.3 - DustTrak data
Test 1
Test 2
Test 3
Conc.(mg/cm³)
Time (mm:ss)

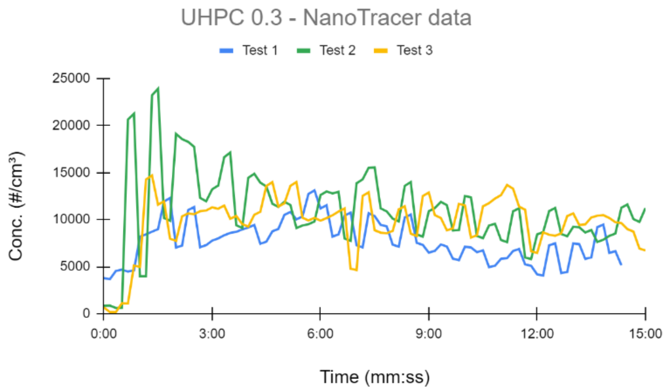
UHPC 0.3 - NanoTracer data
Test 1
Test 2
Test 3
Conc. (#/cm³)
Time (mm:ss)

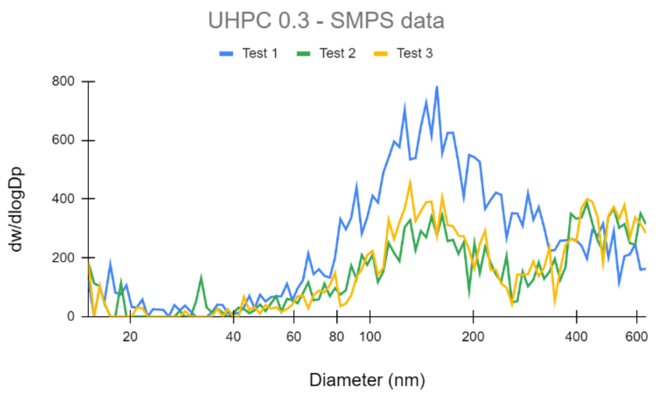
UHPC 0.3 - SMPS data
Test 1
Test 2
Test 3
dw/dlogDp
Diameter (nm)

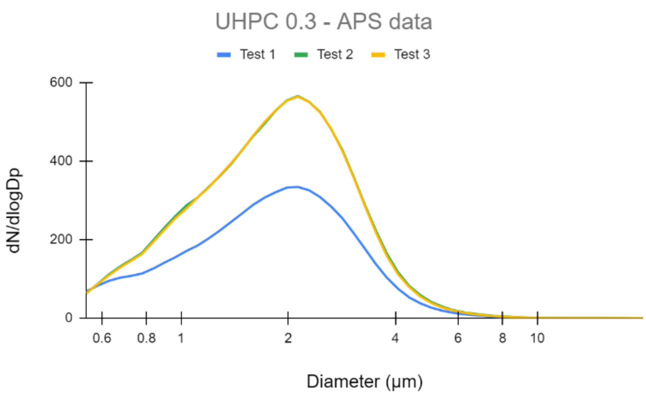
UHPC 0.3 - APS data
Test 1
Test 2
Test 3
dN/dlogDp
Diameter (μm)

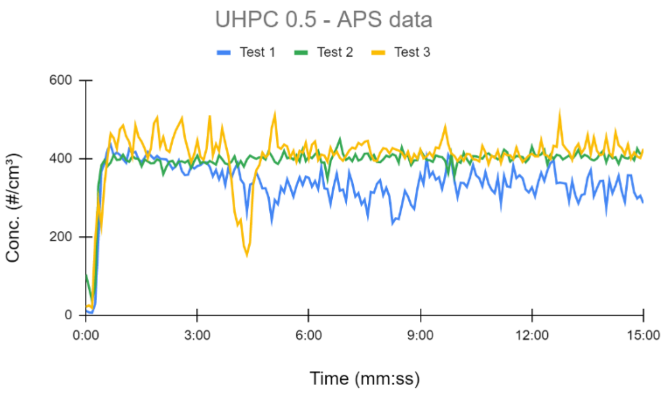
UHPC 0.5 - APS data
Test 1
Test 2
Test 3
Conc. (#/cm³)
600
400
200
0
0:00
3:00
6:00
9:00
12:00
15:00
Time (mm:ss)

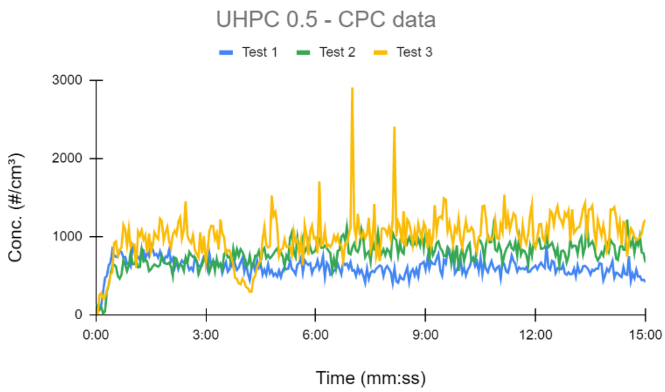
UHPC 0.5 - CPC data
Test 1
Test 2
Test 3
Conc. (#/cm³)
3000
2000
1000
0
0:00
3:00
6:00
9:00
12:00
15:00
Time (mm:ss)

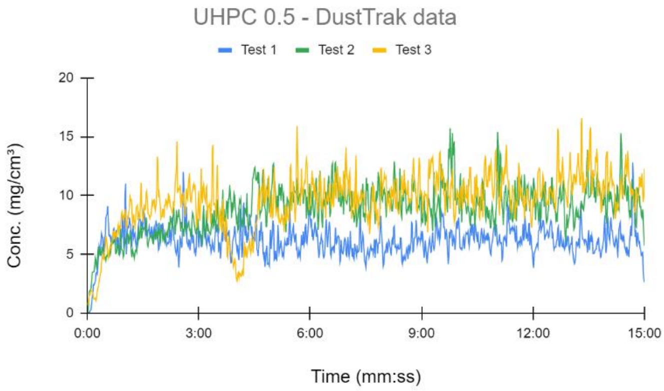
UHPC 0.5 - DustTrak data
Test 1
Test 2
Test 3
Conc. (mg/cm³)
20
15
10
5
0
0:00
3:00
6:00
9:00
12:00
15:00
Time (mm:ss)

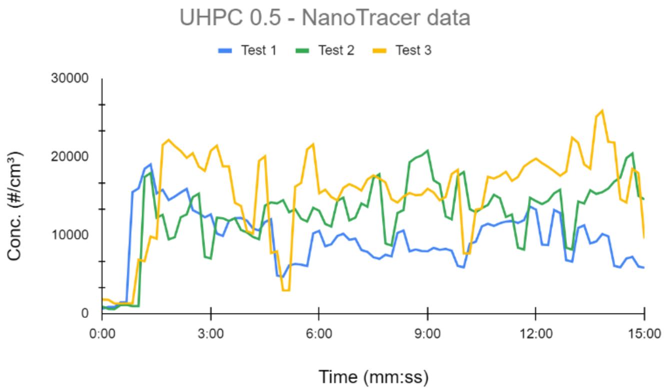
UHPC 0.5 - NanoTracer data
Test 1
Test 2
Test 3
Conc. (#/cm³)
30000
20000
10000
0
0:00
3:00
6:00
9:00
12:00
15:00
Time (mm:ss)

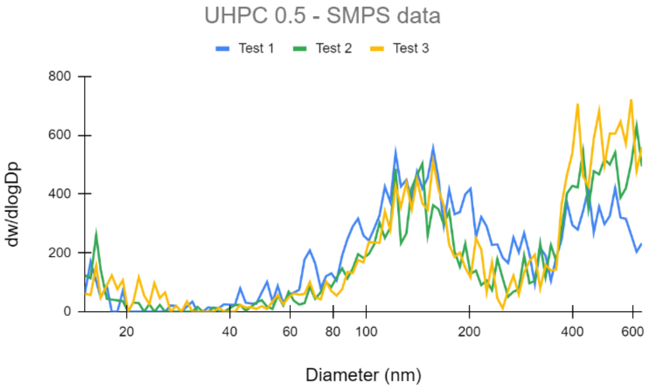
UHPC 0.5 - SMPS data
Test 1
Test 2
Test 3
dw/dlogDp
800
600
400
200
0
20
40
60
80
100
200
400
600
Diameter (nm)

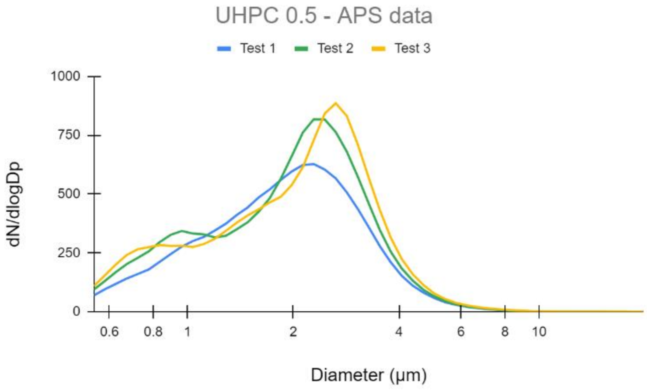
UHPC 0.5 - APS data
Test 1
Test 2
Test 3
dN/dlogDp
1000
750
500
250
0
0.6
0.8
1
2
4
6
8
10
Diameter (µm)

Appendix B

Sample type	Fallen mass (g)	Retained mass (g)	Start mass (g)	Respirable (mg/m^3)	Total (mg/m^3)
NSC 0 – 1	6.9	93.4	100	-*	38.7
NSC 0 – 2	12.6	83.8	100	4.30	56.0
NSC 0 – 3	13.1	86.4	100	1.78	11.4
NSC 0.05 – 1	15.1	68.8	89	4.45	78.3
NSC 0.05 – 2	13.5	74.5	89	-*	105.2
NSC 0.05 – 3	15.1	72.6	89	3.85	12.9
NSC 0.1 – 1	16.9	40.6	60	5.82	32.2
NSC 0.1 – 2	18.3	40.2	60	7.64	24.2
CLC 0 – 1	31.0	70.3	100	9.85	206.9
CLC 0 – 2	31.9	66.6	100	11.3	280.4
CLC 0 – 3	34.0	64.2	100	12.7	486.1
CLC 0.1 – 1	18.2	78.8	100	2.85	200.9
CLC 0.1 – 2	17.9	80.6	100	3.59	175.7
CLC 0.1 – 3	18.9	79.3	100	3.50	31.2
CLC 0.3 – 1	15.6	79.9	98	4.55	232.7
CLC 0.3 – 2	16.4	79.3	98	5.35	291.8
CLC 0.3 – 3	15.0	79.4	98	2.53	268.1
UHPC 0 – 1	20.0	77.9	100	4.59	242.2
UHPC 0 – 2	18.1	81.4	100	7.80	144.7
UHPC 0 – 3	17.7	81.0	100	9.16	43.7
UHPC 0.3 – 1	13.5	84.3	100	5.72	208.3
UHPC 0.3 – 2	18.4	80.3	100	5.01	163.9
UHPC 0.3 – 3	17.6	81.1	100	2.53	124.4
UHPC 0.5 – 1	20.7	54.6	77	4.01	167.9
UHPC 0.5 – 2	21.9	54.4	77	9.64	330.0
UHPC 0.5 – 3	20.2	56.0	77	9.51	40.8

*No calculated concentration as the sampled mass on the filter was too low to be detected.

Appendix C

	(particles/cm^3)						(mg/cm^3)	
	APS		CPC		NT		DT*	
Sample type	μ	σ	μ	σ	μ	σ	μ	σ
NSC 0 – 1	66.5	25.6	209.7	73.2	2200	1194	4.05	3.03
NSC 0 – 2	92.2	11.9	226.5	42.2	4197	1650	4.72	1.38
NSC 0 – 3	92.2	13.5	216.6	39.2	4700	1435	4.56	1.01
NSC 0.05 – 1	136.1	18.8	323.2	51.7	6830	2164	6.89	2.23
NSC 0.05 – 2	110.9	18.3	245	46.6	8644	2583	4.51	1.29
NSC 0.05 – 3	121.9	19.8	231.4	45.8	5342	2133	5.01	1.18
NSC 0.1 – 1	437.6	54.9	831.2	552.8	54035	10554	-	-
NSC 0.1 – 2	468	65.3	999.9	207	77598	18398	-	-
CLC 0 – 1	422.6	33.1	1051.5	361.6	35439	15396	23.7	6.38
CLC 0 – 2	445.5	16.3	1455.9	315.2	29538	7040	28.9	11.96
CLC 0 – 3	455.5	27.2	1904.3	727.9	26672	5717	19.8	3.97
CLC 0.1 – 1	155.5	19.8	493.2	92.7	3467	1408	13.3	5.02
CLC 0.1 – 2	156.7	14.6	425.1	126	2436	500	10.7	2.52
CLC 0.1 – 3	175.3	18.4	417	81.1	2056	374	7.94	2.59
CLC 0.3 – 1	145.3	16.3	358.3	72	2335	497	8.84	3.01
CLC 0.3 – 2	142.2	14.3	317.5	318.8	2792	511	11.6	3.71
CLC 0.3 – 3	155.3	14.6	332.9	63.4	3495	673	7.91	2.95
UHPC 0 – 1	398.8	20.9	833.5	145.8	21097	3862	8.82	1.58
UHPC 0 – 2	379.4	19.8	897	162.8	8586	3097	7.36	1.36
UHPC 0 – 3	396.6	25.6	1082.1	266.3	14501	3140	8.23	1.25
UHPC 0.3 – 1	376.6	28	430.8	100.1	7846	2080	4.77	1.26
UHPC 0.3 – 2	306	34.6	480.4	91.3	10730	2565	6.66	1.27
UHPC 0.3 – 3	294.6	34.9	448.1	211.6	10330	1947	7.21	1.65
UHPC 0.5 – 1	340.5	38.6	593.7	81.6	9227	2290	6.19	1.07
UHPC 0.5 – 2	400.2	13.1	832.7	117.5	13837	3091	9.53	1.49
UHPC 0.5 – 3	414.7	48.8	1037.1	277.9	16333	4320	10.01	2.07

μ: mean concentration, σ: standard deviation

*PM4 fraction was measured with the DT

Appendix D

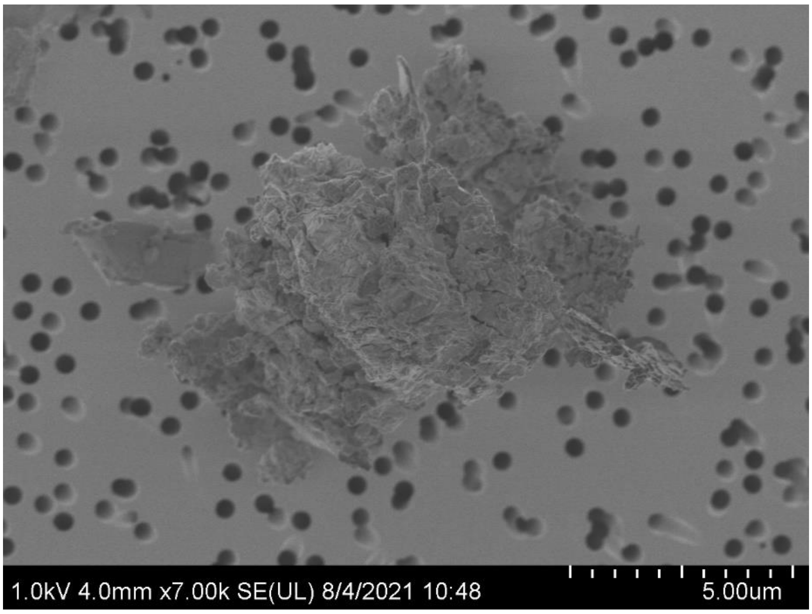

Figure A.0.1 Normal strength concrete without carbon nanotubes.

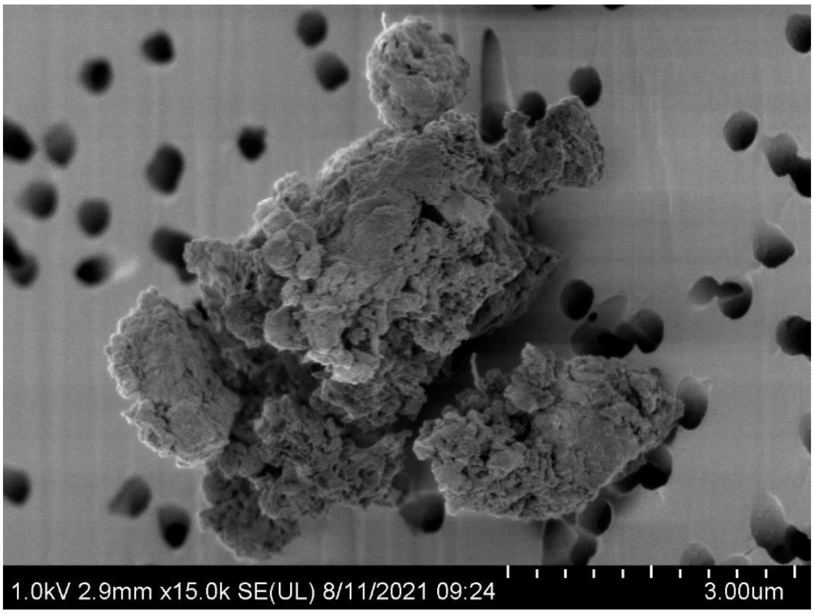

Figure A.0.2 Normal strength concrete with 0.1 wt% carbon nanotubes.

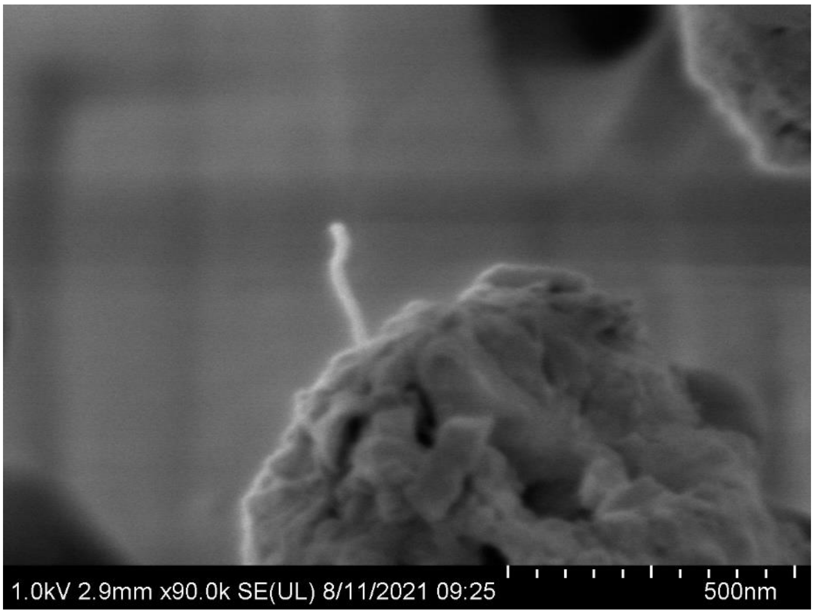

Figure A.0.3 Close-up of carbon nanotube from the normal strength concrete containing 0.1 wt% carbon nanotubes.

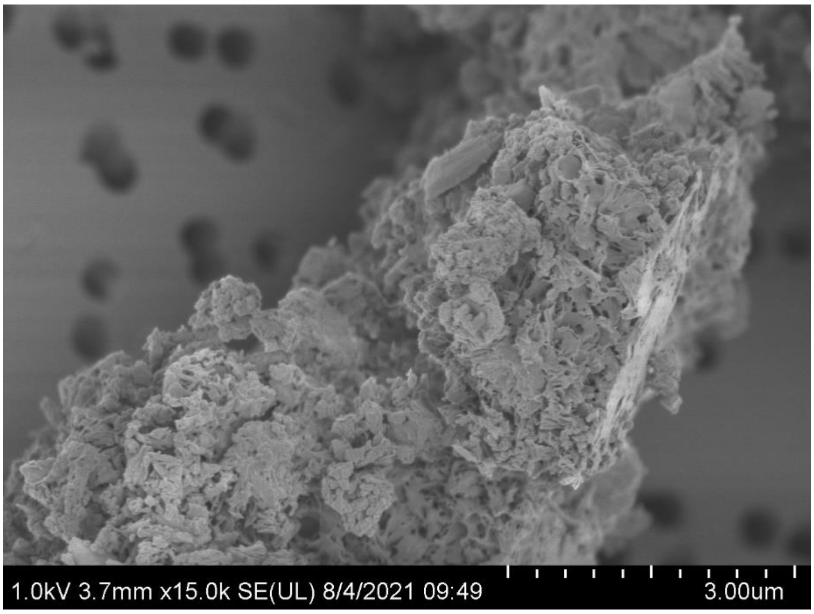

Figure A.0.4 Particle from the CLC without carbon nanotubes.

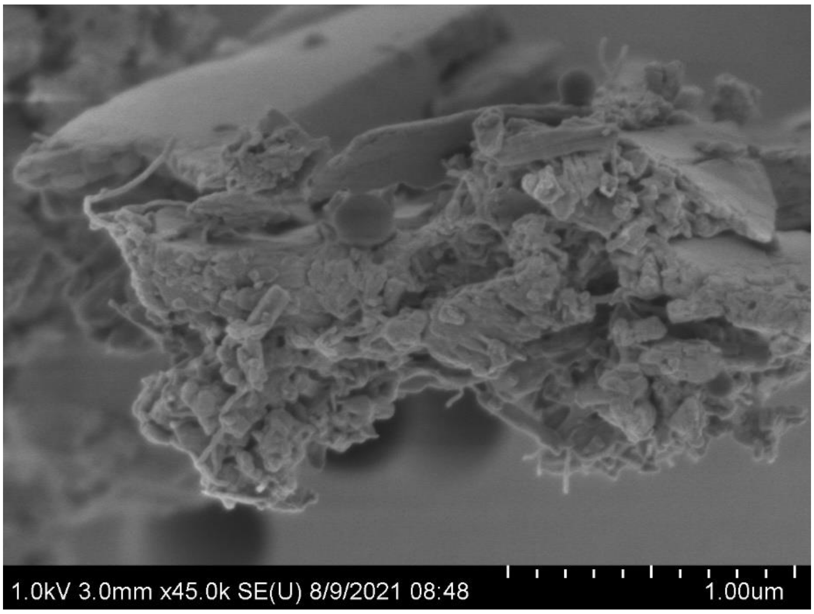

Figure A.0.5 Particle from the CLC containing 0.3 wt% carbon nanotubes.

Appendix E

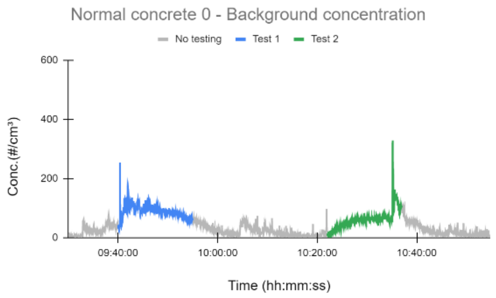
Normal concrete 0 - Background concentration
No testing
Test 1
Test 2
Conc. (#/cm³)
Time (hh:mm:ss)

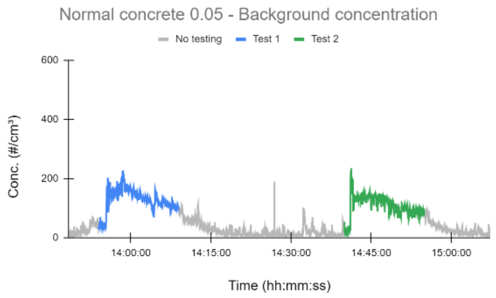
Normal concrete 0.05 - Background concentration
No testing
Test 1
Test 2
Conc. (#/cm³)
Time (hh:mm:ss)

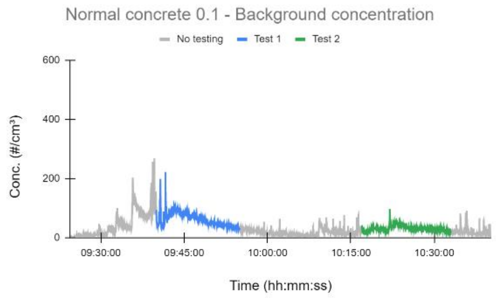
Normal concrete 0.1 - Background concentration
No testing
Test 1
Test 2
Conc. (#/cm³)
Time (hh:mm:ss)

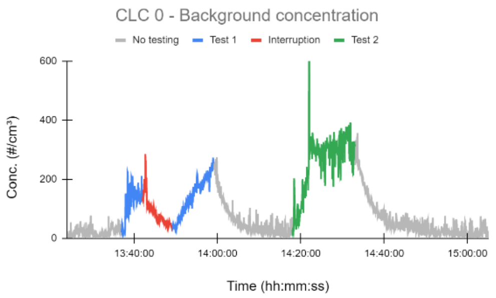
CLC 0 - Background concentration
No testing
Test 1
Interruption
Test 2
Conc. (#/cm³)
Time (hh:mm:ss)

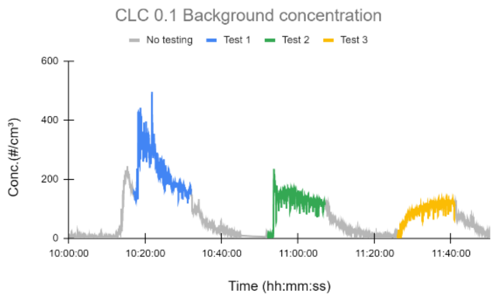
CLC 0.1 Background concentration
No testing
Test 1
Test 2
Test 3
Conc. (#/cm³)
Time (hh:mm:ss)

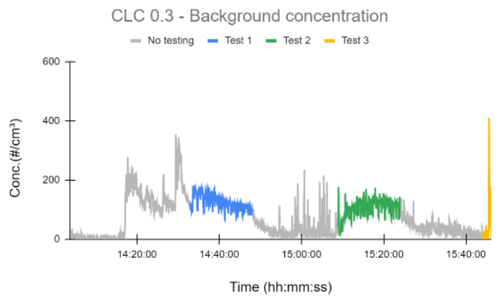
CLC 0.3 - Background concentration
No testing
Test 1
Test 2
Test 3
Conc. (#/cm³)
Time (hh:mm:ss)

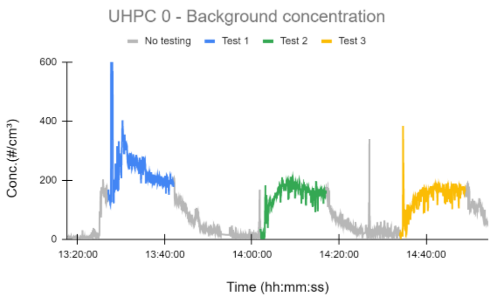
UHPC 0 - Background concentration
No testing
Test 1
Test 2
Test 3
Conc. (#/cm³)
Time (hh:mm:ss)

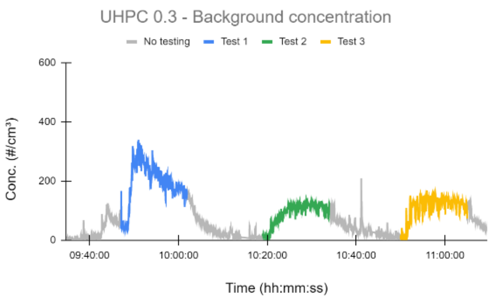
UHPC 0.3 - Background concentration
No testing
Test 1
Test 2
Test 3
Conc. (#/cm³)
Time (hh:mm:ss)

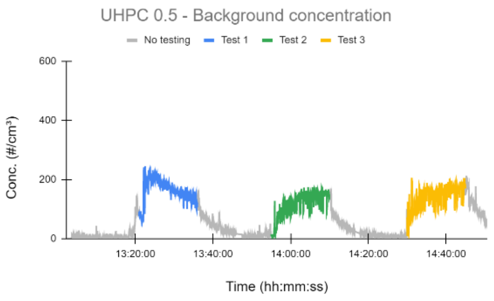
UHPC 0.5 - Background concentration
No testing
Test 1
Test 2
Test 3
Conc. (#/cm³)
Time (hh:mm:ss)

Appendix F

Risk analysis of dustiness testing of crushed CNT-enhanced concrete in the aerosol lab

Description of experiment

Dustiness testing of crushed concrete containing different weight percentages of carbon nanotubes will be performed in the aerosol exposure chamber at IKDC. The crushed concrete will be dropped in a closed cylinder according to a standard method (continuous drop method, EN 15051-3) and the resulting airborne emissions will be sampled. The aim is to characterize the emitted particles and compare the fraction of the CNTs in different particle sizes of the aerosol to the different weight percentages in the bulk material. Measurements and characterisation of these particles will contribute to understanding of the risks associated with using concrete enhanced with engineered nanoparticles during construction as well as at later stages in the life cycle of the materials, where concrete structures are demolished (Lee et al., 2010).

CNTs can be dispersed in concrete to alter the material properties, where their high tensile strength and large surface area helps prevent crack propagation, thus improving the mechanical properties and durability of concrete. They also have excellent electrical properties and high conductivity, which could possibly be used for monitoring the structural health of concrete materials (García-Macías, 2017). However, the potential health risks associated with addition of CNTs in construction may offset the benefits (Lee et al, 2010), which motivates further studies on their behaviour and toxicity when used as additions in construction applications.

Place: Exposure chamber in aerosol lab
Dates: April - May 2021
Personnel: Sara Marsh, Camilla Abrahamsson

Instruments:
CPC
SMPS
APS
Nanotracer
DustTrak
Filter samples for SEM and gravimetric analysis

Identification of risks

The main risks identified with the experiments are presented in Table 1 below.

Table 1. Main risks with the experiments and how to avoid them.

Risk	Can be caused by	How will risk be avoided
The surrounding lab air gets contaminated by CNTs	**1.** Wrong setting on chamber ventilation so that overpressure occurs in the chamber	**1.** Continuously monitor and maintain an underpressure of 5-10 Pa by connecting a U-tube to the chamber. Establish which settings for the ventilation should be used to maintain the underpressure.
	2. Crushed concrete released from storage containers during transport to the chamber	**2.** Use tape as an extra seal on the storage containers to keep them from opening if dropped.
	3. Residual contamination on person in the chamber after protective gear has been taken off	**3.** Written routines on how to safely remove protective gear in the ante chamber before exiting. Glasses and mask will be transported in a box to a fume hood and cleaned. Make sure the tape at the ante chamber floor is fresh and sticky. Only removing waste container from fume hood

		after ensuring that the lid is firmly sealed and the outside has been cleaned.
Inhalation of CNTs by person in chamber	Respiratory protection (mask) not tight fitting enough around the face. Residual contamination of the mask from earlier experiments.	Ensure tight fit before entering the chamber. Masks should be wiped on the inside and outside with 70% ethanol after use (new wipes for inside and outside).
Contamination of the chamber	**1.** Cylinder breaking, leaking or malfunctioning due to overpressure in the cylinder (wrong settings on instruments or vacuum). **2.** Collected crushed concrete is released by accident when filters are removed or when concrete is transferred to the weighing container.	**1**.Written checklist on the settings of the different instruments which shall be checked thoroughly before an experiment starts. If release happens: start express ventilation and let it run for 10 minutes while the person remains in the chamber. Then clean surfaces with 70% ethanol (reduce the amount of concrete particles present in the chamber before continuing with experiments). **2.** Practice proper handling of filters and collected concrete (with non-CNT-containing crushed concrete before CNT-containing concrete is used) to ensure that the person doing

	the experiments is confident in how to remove them safely. Have ethanol and wipes in the chamber to handle spills. Lab coats will be kept in the chamber entrance and cleaned (or disposed of) after the experiments.
3. Cleaning of the inner tube results in release of large amounts of crushed concrete into the chamber air.	**3**. All cleaning should be as wet as possible (70% ethanol) and the brush/wipes should be stored in a sealed box inside the chamber.

Exposure chamber and experiment set-up

The set-up will be calibrated and tested using crushed concrete without added CNT before CNT-containing samples are tested. The concrete without CNTs is already sifted into different size fractions (4 mm, 2 mm, 1 mm, 0.5 mm, 0.250 mm, 0.125 mm). Different size fractions will be tested through trial and error during the calibration stage to find out which sizes work with the set-up, so the final size fraction is not yet known at the stage of the risk analysis. The results of this will govern to which size fractions of CNT-containing crushed concrete will be sifted.

The sifting process is a potential source for contamination of the surrounding air as the crushed concrete will be shaken, so the sifting will be performed in a well ventilated fume hood. PPE (mask, protective glasses and gloves) will be worn by the person performing the sifting.

The set-up for the continuous drop-method (European Standard EN 15051-3) will consist of a stainless steel cylinder with 150 mm in diameter and 1100 mm in height. The container will have an inlet for back-flow (53 l/min) and six sampling outlets connected to filters and online instruments. The air flow through the filters will be driven by the vacuum system in the lab. The crushed concrete will be fed through a pipe 25 mm in diameter into the cylinder from above by a rotating arm. The fallen concrete will be collected at the bottom of the cylinder, transferred to a smaller weighing container by the person in the chamber and then be transported to the outside in tightly sealed containers. Since weighing has been recognized as a work procedure with high risk of airborne exposure to engineered nanomaterials (Johnson et al., 2010), the crushed concrete will be in sealed containers with predetermined weights during their weighing to avoid contaminating the weighing room or exposing personnel.

The conditions in the chamber will be set to a temperature of 21 °C (± 3) and a relative humidity (RH) of 50 % (± 10) according to the testing method standard (EN 15051-3). An underpressure of 5-10 Pa will be maintained during the experiments to contain unexpected concrete leaks within the chamber. The outlets from the chamber will be tightly sealed with duct tape around the metal tubes connecting the inside of the chamber with the surrounding lab environment. HEPA-filters will be also installed on all chamber ventilation outlets.

Personnel and guests will be informed of the ongoing experiment through a warning sign on the chamber door (“Ongoing CNT emission study, do not enter”) and there will also be some public information for people that may be concerned at a lab meeting.

Since cleaning is a work process which has been shown to have increased risk of exposure to carbon nanotubes in industrial settings (Hedmer et al., 2014), the cleaning of the cylinder between concrete types is a critical step. The tube through which the crushed concrete falls down into the cylinder will be the most contaminated area and it will be cleaned with a small brush and rinsed with 70 % ethanol. The collected waste will be disposed of in a sealed container and treated as hazardous waste. The cylinder will be flushed with clean air in between experiments.

The concrete

Three different types of concrete will be tested: “regular” concrete, Cellular Lightweight Concrete (CLC) and Ultra High Performance Concrete (UHPC). These types of concrete have slightly different properties and uses. For each type there will be one sample without CNTs (for calibration and reference) and two samples with different weight percentages of CNT. All concrete types are presented in Table 2 below.

Table 2: Concrete samples used in the experiments.

Concrete type	Fraction CNTs (wt%)	Density (kg/m3)
"Regular" concrete	Sample 0: - Sample 1: 0.05 Sample 2: 0.1	2187
CLC	Sample 0: - Sample 1: 0.1 Sample 2: 0.3	300
UHPC	Sample 0: - Sample 1: 0.3 Sample 2: 0.5	2350

Since each experiment requires a maximum of 100 g material, approximately 4.05 g (1.35 x 3 times) CNTs in total will be used in the experiments.

According to the standard, a sample of crushed concrete will be continuously dropped during 10 minutes and then collected concrete will be weighed. The crushed concrete will be collected on a removable tray at the bottom of the container and the contents will be transferred to a marked and sealed container for safe gravimetric weighing in the lab. This will be repeated two times after the first test to enable statistical analysis of the results. Filters will be exchanged in between experiments and these will be removed and sealed shut and then the casing will be cleaned with 70 % ethanol.

The crushed concrete will be placed in airtight containers between experiments and only opened within the chamber to avoid contamination of the lab or personal exposure. The containers will be marked with labels, stored in a locked cabinet to ensure that no one opens them by mistake and sealed with tape to avoid unintentional opening outside of the exposure chamber. Excess dust will be stored in their marked containers in a locked cabinet after use.

There are some health risks associated with inhalation of concrete dust in itself. Crystalline silica is a component in stone, which is used in concrete as ballast. Inhalation of crystalline silica can cause adverse health effects in humans, including lung cancer and silicosis according to WHO (2000). These studies were mainly done on workers exposed to respirable crystalline silica for several years (Park, 2019), but short-term exposure tests in rats also showed that inhalation of crystalline silica could be linked to pulmonary inflammation and damage the macrophage clearance functions (Meijer, 2001).

The carbon nanotubes

The CNTs used in the experiments are multiwalled of the type NC7000 and have an average diameter of 9.5 nm and an average length of 1.5 µm. The carbon purity is 90 % and they contain <1 % transition metal oxides.

Currently there are no occupational exposure limits in place for CNTs (Thompson et al., 2015), but a number of studies have raised concerns about their ability to cause damage in the lung when inhaled. One type of CNTs (Mitsui-7 CNTs) are classified as carcinogenic to humans (Grosse et al., 2014). Mitsui-7 CNTs have a tube diameter of 40-90 nm and a tube length of 5.7 ± 0,49 µm according to the manufacturer, although slight differences in dimensions have been noted when they have been used in research (Rahman et al., 2017). As mentioned previously, the carbon nanotubes in these experiments will be both much thinner and shorter than the Mitsui-7 CNTs, possibly making them less hazardous.

Carbon nanomaterials are in general hydrophobic, which makes them difficult to disperse in physiological environments. The high surface area of the nanoparticles and the cylinder shape means that there is potential for the nanotubes to adsorb biomolecules or other small molecules which could disturb biological processes (Sanchez et. al., 2009). Surface modifications or residual metal catalysts from the synthesis of CNTs can also be a cause for potential health risks. Transition metals such as iron, nickel or yttrium are often used as catalysts when CNTs are produced and they can cause the formation of reactive species, such as iron saccharate, which has been shown to induce sarcomas in rats. Since no purification process is 100 % effective, even pure nanotubes will likely contain residual metals (Sanchez et. al., 2009).

Long CNT fibers have been shown to produce inflammation and fibrosis responses in the peritoneal cavity in a similar fashion to asbestos (Donaldson et al., 2010; Nakanishi et al., 2015). They also cause oxidative stress which can be a risk factor for pulmonary cancer (Nakanishi et al., 2015). The high aspect ratio of CNTs enables them to reach beyond the ciliated airways in the lung, to where phagocytosis occurs. If the fibers are longer than the diameter of the macrophages (10-20 µm) they will not be removed effectively and can cause frustrated phagocytosis and oxidative stress (Sanchez et. al., 2009). Fibers deposited in the respiratory organs that are difficult to clear or break down are likely to accumulate in the body and have a high biopersistence. Although the NC7000 CNTs are relatively short, they can agglomerate and form longer rope-like structures (Wick et. al., 2007).

CNTs often agglomerate due to their geometry and hydrophobic surface to form bundles (Lam et al., 2004; Thompson et al., 2015). This can affect the toxicity, since the aerodynamic diameter is changed (Donaldson et al., 2010; Wick et al. 2007), thus changing where an inhaled fiber will deposit in the lung (Kreyling et al., 2007). It is not completely established how the degree of agglomeration affects the toxicity, but it has been suggested that agglomerates are more toxic than well-dispersed nanotubes (Sanchez et. al., 2009). It is however, important to keep in mind the heterogeneity of CNTs as they can differ in dimensions, purification, modifications and degree of agglomeration. Furthermore, how this agglomeration process is affected by the dispersion in concrete which is then crushed is not known. As of today, it has not been studied if or how the dispersion of CNTs in crushed concrete affects the toxicity or how the toxicity of crushed concrete in itself is modified by the addition of CNTs.

Personal protective equipment (PPE)

Personnel working with CNT-containing crushed concrete may be exposed through inhalation but exposure through the skin and eyes are also possible routes. To prevent this, personnel working in the chamber will be using the following PPE (in accordance with the Safety Data Sheet for NC7000 CNTs)

- Disposable nitrile gloves (double)
- Respirator with particle filter
- Tight-fitting protective glasses
- Lab coats and pants
- Disposable shoe covers

PPE (mask and protective glasses) will be placed in a sealed plastic box, transported to a fume hood and wiped down with 70% ethanol immediately after experiments are finished. The nitrile gloves and shoe covers will be disposed of in a plastic bag which will be placed in a sealed box for waste. Lab coats will be kept in the ante chamber to prevent contamination of the lab. Personnel who has been in the chamber should also wash hands and face thoroughly afterwards.

In addition, an online instrument will be placed in the chamber to continuously measure the background particle concentration.

Instruments and filters

Filters will be placed on all instrument exhausts to ensure no leakage of CNTs in the lab. After the experiments the filters will be removed and labeled with CNT to ensure proper disposal.

Waste handling and cleaning after finished experiments

After all measurements are done, the surfaces in the chamber will be cleaned using disposable wipes and 70% ethanol. The wipes will be treated as hazardous material and disposed of in a sealed box. The same PPE that is used during the experiments will also be used during the cleaning of the exposure chamber. HEPA-filters on chamber outlets will be discarded as hazardous waste.

The instruments (as well as the filters on instrument exhausts) will be marked with stickers describing that they have been used in experiments on CNTs. Tubes used with the instruments will be discarded when all measurements are completed. The cylinder container will be cleaned and stored in a sealed and marked box for future experiments.

The experiments will generate waste in the form of tubing, cleaning wipes, nitrile gloves, shoe covers and filters. Lab coats will be disposed of. The waste will be disposed of in sealed plastic boxes, which will be stored in a locked cabinet until hazardous waste from the aerosol lab is collected. The boxes containing waste will be marked with their content, explicitly stating that the boxes contain CNT-contaminated waste. Surplus concrete that cannot be used in future experiments will be disposed of by placing it in closed containers in the waste box.

References

Donaldson, K., Aitken, R., Tran, L., Stone, V., Duffin, R., Forrest, G., Alexander, A. (2006) Carbon Nanotubes: A Review of Their Properties in Relation to Pulmonary Toxicology and Workplace Safety, *Toxicological Sciences*, 92(1), pp: 5–22. doi: 10.1093/toxsci/kfj130

Donaldson, K., Murphy, F.A., Duffin, R. *et al*. (2010) Asbestos, carbon nanotubes and the pleural mesothelium: a review of the hypothesis regarding the role of long fibre retention in the parietal pleura, inflammation and mesothelioma. *Particle and Fibre Toxicology*, 7(5). doi: 10.1186/1743-8977-7-5

García-Macías, E., D'Alessandro, A., Castro-Triguero, R., Pérez-Mira, D., Ubertini, F., (2017) Micromechanics modeling of the electrical conductivity of carbon nanotube cement-matrix composites, *Composites Part B: Engineering*, 108, pp: 451-469, doi: 10.1016/j.compositesb.2016.10.025

Grosse, Y., Loomis, D., Guyton, K. Z., Lauby-Secretan, B., El, G. F., Bouvard, V., . . . Straif, K. (2014). Carcinogenicity of fluoro-edenite, silicon carbide fibres and whiskers, and carbon nanotubes. *Lancet Oncological*, 15, pp: 1427-1428. doi:10.1016/S1470-2045(14)71109-X

Hedmer, M., Isaxon, C., Nilsson, P. T., Ludvigsson, L., Messing, M. E., Genberg, J., . . . Pagels, J. H. (2014). Exposure and emission measurements during production, purification, and functionalization of arc-discharge-produced multi-walled carbon nanotubes. *Annals of Occupational Hygiene, 58,* 355- 379. doi:10.1093/annhyg/met072

Johnson, D. R., Methner, M. M., Kennedy, A. J., & Steevens, J. A. (2010). Potential for Occupational Exposure to Engineered Carbon-Based Nanomaterials in Environmental Laboratory Studies. *Environmental Health Perspectives*, *118*(1), 49–54. https://doi.org/10.1289/ehp.0901076

Jung, M., Lee, Y.-soon, Hong, S.-G., & Moon, J. (2020). Carbon nanotubes (CNTs) in ultra-high performance concrete (UHPC): Dispersion, mechanical properties, and electromagnetic interference (EMI) shielding effectiveness (SE). *Cement and Concrete Research*, *131*, 106017. https://doi.org/10.1016/j.cemconres.2020.106017

Kreyling, W. G., Moller, W., Semmler-Behnke, M., & Oberdorster, G. (2007). Particle dosimetry: Deposition and clearance from the respiratory tract and translocation to extra-pulmonary sites. In K. Donaldson, & P. Borm, Particle toxicology (ss. 47-74). CRC Press.

Lam, C.W., James, J.T., McCluskey, R., Hunter, R.L. (2004) Pulmonary toxicity of single-wall carbon nanotubes in mice 7 and 90 days after intratracheal instillation, *Toxicological Sciences*, *77(1)*, 126-134. doi: 10.1093/toxsci/kfg243.

Lee, J., Mahendra, S., & Alvarez, P. J. (2010). Nanomaterials in the Construction Industry: A Review of Their Applications and Environmental Health and Safety Considerations. *ACS Nano*, *4*(7), 3580–3590. https://doi.org/10.1021/nn100866w

Meijer, E., Kromhout, H., & Heederik, D. (2001) Respiratory effects of exposure to low levels of concrete dust containing crystalline silica, *American Journal of Industrial Medicine, 40(2),* pp:133-40. doi: 10.1002/ajim.1080.

Mohsen, M., Alansari, M., Taha, R., Senouci, A., Abutaqa, A., (2020) Impact of CNTs' treatment, length and weight fraction on ordinary concrete mechanical properties, *Construction and Building Materials*, *264,* 120698. https://doi.org/10.1016/j.conbuildmat.2020.120698.

Nakanishi, J., Morimoto, Y., Ogura, I., Kobayashi, N., Naya, M., Ema, M., . . . Hanai, S. (2015). Risk assessment of the carbon nanotube group. *Risk Analysis, 35(10),* 1940-1956. doi:10.1111/risa.12394

Park, H., Hwang, E., & Yoon, C. (2019). Respirable Crystalline Silica Exposure among Concrete Finishing Workers at Apartment Complex Construction Sites. *Aerosol and Air Quality Research, 19*, 2804-2814.

Rahman, L., Jacobsen, N. R., Aziz, S. A., Wu, D., Williams, A., Yauk, C. L., … Halappanavar, S. (2017). Multi-walled carbon nanotube-induced genotoxic, inflammatory and pro-fibrotic responses in mice: Investigating the mechanisms of pulmonary carcinogenesis. *Mutation Research/Genetic Toxicology and Environmental Mutagenesis*, *823*, 28–44. https://doi.org/10.1016/j.mrgentox.2017.08.005

Sanchez, V.C., Pietruska, J.R., Miselis, N.R., Hurt, R.H. and Kane, A.B. (2009), Biopersistence and potential adverse health impacts of fibrous nanomaterials: what have we learned from asbestos?. WIREs Nanomed Nanobiotechnol, 1: 511-529. https://doi.org/10.1002/wnan.41

Thompson, D., Chen, S.-C., Wang, J., & Pui, D. Y. H. (2015). Aerosol Emission Monitoring and Assessment of Potential Exposure to Multi-walled Carbon Nanotubes in the Manufacture of Polymer Nanocomposites. *Annals of Occupational Hygiene*, *59*(9), 1135–1151. https://doi.org/10.1093/annhyg/mev044

World Health Organization & International Programme on Chemical Safety. (2000). Crystalline silica, quartz. World Health Organization. https://apps.who.int/iris/handle/10665/42297

Wick, P., Manser, P., Limbach, L., Dettlaff-Weglikowska, U., Krumeich, F., Roth, S., … Bruinik, A. (2007). The degree and kind of agglomeration affect carbon nanotube cytotoxicity. *Toxicology Letters*, *168*(2), 121–131. https://doi.org/10.1016/j.toxlet.2006.08.019